Summer 8-13-2021

The Staphylococcus Aureus lrgAB Operon Encodes a Holin-Like Protein Involved in Pyruvate Transport

Jennifer L. Endres
University of Nebraska Medical Center

The *Staphylococcus aureus lrgAB* operon encodes a holin-like protein involved in pyruvate transport

By

Jennifer Leigh Endres

Presented to the Faculty of

The University of Nebraska Graduate College

In Partial Fulfillment of the Requirements

for the Degree of Master of Science

Immunology, Pathology & Infectious Disease
Graduate Program

Under the Supervision of Professor Kenneth W. Bayles

University of Nebraska Medical Center
Omaha, NE

June, 2021

Advisory Committee:

Paul D. Fey, Ph.D.

Vinai C. Thomas, Ph.D.

The *Staphylococcus aureus lrgAB* operon encodes a holin-like protein involved in pyruvate transport

Jennifer L. Endres, M.S.

University of Nebraska, 2021

Advisor: Kenneth W. Bayles, Ph.D.

The *Staphylococcus aureus cidABC* and *lrgAB* operons encode a well-conserved family of proteins involved in programmed cell death (PCD) during biofilm development. Based on the structural similarities that CidA and LrgA share with bacteriophage holins, we have hypothesized that these proteins function by forming pores within the cytoplasmic membrane. To test this, we utilized a "lysis cassette" system that demonstrated the abilities of the *cidA* and *lrgA* genes to support bacteriophage endolysin-induced cell lysis. In addition, the CidA and LrgA proteins were shown to localize to the surface of membrane vesicles and cause leakage of small molecules, providing direct evidence of their channel-forming potential. Consistent with recent reports demonstrating a role for the *lrgAB* operon in the transport of byproducts of carbohydrate metabolism. We also show that *lrgA* and *lrgB* are important for *S. aureus* to utilize pyruvate during growth with pyruvate as the sole carbon source. A growth defect is observed when the *lrgAB* mutant is grown under microaerobic and anaerobic conditions where *S. aureus* does not utilize amino acids leading to a necessity for the import of pyruvate for energy production. Additionally, the LytSR two-component regulatory system, which induces the *lrgAB* operon, responds to weak acid stress as well as dissipation of membrane potential. In agreement with these findings, mutations in components of the electron transport chain lead to higher expression of *lrgAB* via LytSR regulation. Finally, recent research in *Streptococcus mutans* and

Bacillus subtilis describe a direct role of carbon catabolite regulation of the *lrgAB* homologs and analysis of a *ccpA* mutant in *S. aureus* revealed that it is positive regulator of the *lrgAB* operon. Combined, these data reveal that the CidA and LrgA membrane proteins are functional holins that play an important role in the transport of small byproducts of carbohydrate metabolism.

Table of Contents

Acknowledgements

The research presented in this thesis is a culmination of many years of work that would not have been possible without the help and support of many individuals professionally and personally. The first and foremost person that needs to be acknowledged is my boss and advisor, Dr. Ken Bayles, without his advice and support this work would not have been possible. My ability to critically analyze the bench work and freedom to explore new techniques would not be possible without him. I also have to give a huge thanks to my other committee members, Dr. Paul Fey and Dr. Vinai Thomas who have always been very encouraging. Finally, I have to thank the many graduate and undergraduate students and post-docs that I have been able to work with throughout my scientific career. These individuals have become some of my closest friends and I have learned a lot about myself through the interactions I have had with each and every one of them.

In addition to the individuals who have shaped my scientific career, this would not be possible without the encouragement of my family. To my parents, thank you for always supporting my interests. To my husband, Mike who has always encouraged and given me the chances to do whatever I have wanted, thank you and I love you. I tend to think a lot more can be done in a certain amount of time than in reality can be, and he always figures out how to get my ideas done. And lastly, to my children, Layla and Hayden, your love of life and adventure amazes me, your constant questions about how and why things are/work the way they do keeps me on my toes and reminds me why I love the sciences so much. Without all of these individuals support, I would not be who I am today.

Tables

Figures

Chapter 1 Introduction

Pyruvate metabolism

Pyruvate is the conjugate base of the alpha-keto acid, pyruvic acid. It was identified by Theophile-Jules Pelouze in 1834 by distilling tartaric acid into glutaric acid and an unknown organic acid, later named pyruvic acid [1]. It is a three-carbon molecule that has a ketone and carboxylic acid functional group. Pyruvic acid is a weak acid and has a pKa of 2.93, therefore, when present in a living cell it is primarily found in its dissociated form, pyruvate. Pyruvate is a critical intermediate that sits at the center of many metabolic processes and is the substrate that can branch into different directions during times of excess nutrition or times of distress. Pyruvate unites many key metabolic processes across kingdoms of organisms and the regulation of its availability is an essential part of central metabolism.

In 1926, Kluyver and Donker proposed the unity theory of biochemistry postulating that all living things are identical at the biochemical level [2]. While the enzymatic processes of metabolism are very similar, including common features of hydrogen transfer and the use of high-energy phosphate bonds as a chemical energy source, prokaryotes, eukaryotes, and plants regulate these processes differently. Pyruvate is the compound that sits at the center of all metabolic processes and can provide the necessary building blocks for the cell. It is the end product of glycolysis, the anaerobic metabolism of glucose where two pyruvate molecules are generated per glucose that enters the pathway. During aerobic metabolism, pyruvate can be converted to acetyl-coenzyme A (acetyl-CoA) by pyruvate dehydrogenase (PDH) and enter the tricarboxylic acid cycle (TCA). It is through the TCA cycle that pyruvate is completely decarboxylated to CO_2 [3]. It can be converted to alanine

by an alanine transaminase (ALT) or it can be converted to oxaloacetate by pyruvate carboxylase (PC). During anaerobic growth, pyruvate is converted to lactate by lactate dehydrogenase (LDH). Another key aspect of pyruvate is that it can be converted back into glucose through the gluconeogenesis process. The final fate of pyruvate usage or generation is dictated by the cellular needs at any moment and has high consequences for the cell. For instance, under low oxygen conditions pyruvate can be converted to lactate to regenerate NAD^+ to drive glycolysis, however, only two molecules of adenosine triphosphate (ATP) are generated. Whereas if conditions permit the pyruvate can enter the TCA cycle and the potential to generate 30 ATP arises through oxidative phosphorylation [4].

Staphylococcus aureus pyruvate metabolism

Staphylococcus aureus has the ability to cause disease in many different niches throughout the human host. This is not only due to the vast array of virulence factors that it generates but is also due to its ability to alter its metabolic state. *S. aureus* virulence and metabolism are tightly entwined as expression of many virulence factors results in the release and hydrolysis of host-derived substrates allowing for necessary nutrients to be provided to the cell [5]. *S. aureus* utilizes glycolysis, the TCA cycle and the pentose phosphate pathway to synthesize all of the required central metabolites. One notable aspect of *S. aureus* metabolic pathways is that it lacks a glyoxylate cycle, where acetyl-CoA can enter the TCA cycle through isocitrate but then bypasses two oxidative decarboxylation steps and be converted directly to succinate. The environment plays a key role in the metabolic state of *S. aureus* and the fate of pyruvate.

S. aureus has the ability to grow in both aerobic and anaerobic conditions. The level of oxygen present is one of the largest determinants in the final fate of pyruvate. For instance, when *S. aureus* grows aerobically, glucose is converted to two pyruvate molecules through glycolysis generating two ATP and reducing NAD^+ to NADH. Under these conditions, pyruvate is converted into acetate until all the glucose is consumed. This is due to repression of the TCA cycle by the regulators, CcpA, CodY and SrrA that alter gene expression due to changes in the levels of carbon, nitrogen, and oxygen present in the environment [6, 7]. When glucose is completely consumed the rapid cell growth begins to slow and the cells begin to consume the acetate to provide the acetyl-CoA needed to allow for TCA cycle activity. This change from acetate generation to consumption is referred to as the acetate switch [8]. While the TCA cycle generates another two ATP and biosynthetic intermediates, it also results in reduced dinucleotides. During stationary phase the oxidative phosphorylation that occurs with the electron transport chain oxidizes those dinucleotides so further biosynthetic precursors can be generated.

On the other hand, when *S. aureus* is grown under anaerobic conditions, where it lacks oxygen or another terminal electron acceptor such as nitrate, it will utilize the fermentation of pyruvate to generate necessary energy. Under these conditions the cell relies heavily on the ATP produced through glycolysis. At this point, *S. aureus* utilizes mixed acid fermentation to regenerate the NAD^+ needed to drive further glycolysis and ATP production, resulting in the generation of primarily lactate from pyruvate [9]. When *S. aureus* grows under these conditions less energy is produced than when the cells are respiring.

One of the reasons *S. aureus* is such a significant pathogen is its ability to alter its metabolism depending on the niche with which it is colonized. With pyruvate being a key central metabolite that has the ability to provide the cell with all the essential nutrients for survival, the ability to sense and regulate pyruvate levels within the cell is extremely important to maintain growth and enhance survival. The *S. aureus* genome encodes for regulators that sense and respond to the current catabolic state, nitrogen, oxygen and metal availability, redox state, and TCA cycle activity [10], a subset of these stand out as they play a key role in the fate of pyruvate.

The first set of regulators that have been extremely well characterized are those that belong to the carbon catabolite repression (CCR) family, which includes CcpA and CodY [10]. These regulators allow *S. aureus* to utilize primary carbon sources prior to the utilization of secondary carbon sources. The transcriptional regulator, CcpA, binds to *cre* sites within the promoter regions of genes when the co-repressor, HPr, is phosphorylated and forms the phospho-HPr-CcpA complex [11]. The phosphorylation state of HPr is regulated by HPr kinase, which is activated when the intermediates of glycolysis are present, such as fructose 1,6-bisphosphate as well as glucose 6-phosphate [12]. Due to the repression of TCA cycle genes by CcpA during times of nutrient excess, the pyruvate generated during glycolysis does not enter the TCA cycle through acetyl-CoA. Instead it is converted to acetate through the Pta-AckA pathway [13]. Another important repressor of the TCA cycle that affects the fate of pyruvate in response to amino acid availability is CodY. This regulator affects the expression of over 200 genes and binds to its consensus sequence in the promoter of the genes it regulates due to changes in the branched chain amino acids (BCAA), valine, isoleucine and leucine and to the nucleoside triphosphate

GTP [14]. The generation of these BCAA all start with substrates that are derived from pyruvate, for example isoleucine synthesis begins with oxaloacetate while α-keto-isovalerate is necessary for valine and leucine [7].

Another group of regulators that are encoded within the *S. aureus* genome respond to the redox state of the cell and oxygen availability. As mentioned earlier, *S. aureus* can grow under low oxygen conditions and has the ability to sense and respond to this environment. It is essential as the ability for energy generation through aerobic respiration is decreased in this scenario. The staphylococcal respiratory response AB (SrrAB) proteins are responsible for sensing low oxygen conditions [5]. While the ligand that is sensed by SrrB is unknown, many have speculated that it is menaquinone, a critical part of the electron transport chain [15]. Once SrrB senses the signal, it phosphorylates its cognate response regulator, SrrA that then alters expression of its target genes, including those encoding TCA cycle enzymes, such as NADH dehydrogenase, aconitase, succinate dehydrogenase and fumarase [16]. With the decrease in TCA cycle as well as the electron transport chain, intermediary metabolites are diverted to other pathways such as those that support the biosynthesis of the biofilm matrix molecule, polysaccharide intracellular adhesin (PIA) [17]. In addition to SrrAB, another regulator that affects the fate of pyruvate in *S. aureus* during low O_2 conditions is the redox sensing (NAD^+/NADH ratio) repressor, Rex [18]. In response to increases in the NADH pools from glycolysis and the TCA cycle, the Rex repressor alleviates its repression and allows expression of those enzymes whose activities restore the redox state of the cell. This includes those enzymes within the electron transport chain, those involved in pyruvate to lactate metabolism, and fermentative enzymes.

These regulators are only a few of those known in *S. aureus* and were mentioned because of their regulation of genes that directly affect pyruvate metabolism. Many of these also affect the vast array of *S. aureus* virulence factors that allow for this pathogen to survive under the extreme conditions in which it can cause disease [5]. Thus, it is likely not a coincidence that the regulation of virulence factor expression in *S. aureus* is tied to the regulation of metabolic genes that are important for survival and growth during infection.

Eukaryotes

While pyruvate metabolism in eukaryotic cells is different than what occurs in prokaryotic cells it still remains the key intermediate for the generation of energy, fatty acids and amino acids [4, 19-21]. The biggest difference between eukaryotes and prokaryotes is that in eukaryotes pyruvate generated in the cytosol has to be transported into the mitochondria where it can be metabolized further through the TCA cycle or to oxaloacetate where it can be used for gluconeogenesis [19]. Pyruvate is generated in the cytosol by four different processes, including 1) the breakdown of glucose through glycolysis, 2) the oxidation of lactate by lactate dehydrogenase, 3) the metabolism of malate, and finally, 4) through the metabolism of three carbon amino acids, including alanine, serine, threonine, glycine, cysteine and tryptophan [20]. In order for the cytosolic generated pyruvate to enter the mitochondria it has to pass through three different barriers. First, it must cross the outer mitochondrial membrane, then it has to pass the intermembrane space, and then it must traverse the inner mitochondrial membrane.

Early reports suggested that pyruvate was able to cross the mitochondrial membrane when it was present in its associated, acidic form [19, 20]. One of the biggest

issues with this idea is that the pH of the cell (internal pH 7.2) results in the majority of pyruvate to be in its dissociated, charged form, therefore making a transporter necessary. In the early 1970's, a specific inner mitochondrial membrane protein required for pyruvate transport across the mitochondria membrane in a rat liver was believed to have been identified [22]. Unfortunately, it was later found that this protein was actually an NAD^+ transporter that affected the NAD^+-dependent activity of the pyruvate dehydrogenase [23]. It wasn't until 2012, when two genes, *mpc1* and *mpc2* (originally named BRP44L and BRP44), that encode inner mitochondrial membrane proteins were found to be required for pyruvate transport into the mitochondria [24, 25]. Yeast actually encode a third transporter, *mpc3*, however, only MPC2 or MPC3 along with MPC1 are necessary for pyruvate transport. Because of the arrangement of their promoters, it is speculated that they are induced under different conditions [24]. In yeast, there was no growth defect when *mpc1*, *mpc2* or *mpc3* mutants were grown in nutrient rich media. However, when these same mutants were grown in dextrose media without any amino acids they exhibited growth defects that could be restored by the addition of valine or leucine. Ultimately, ^{14}C pyruvate uptake studies revealed that these genes are necessary for transport of pyruvate across the inner mitochondrial membrane [24, 25]. Subsequently, expression of the eukaryotic *mpc1* and *mpc2* in *Lactococcus lactis* allowed for the uptake of the labelled pyruvate [24], providing additional support that these genes are required for pyruvate import.

Characterization of these proteins revealed that MPC1 and MPC2 are relatively small and have a molecular mass of 12- and 15- kDa, respectively. These proteins are predicted to have three transmembrane domains each and form a heteromeric complex of roughly 150- kDa in the inner mitochondrial membrane [25]. MPC1 does not have the

ability to oligomerize with itself unless MPC2 is present to form the heteromeric complex. Although purified MPC2 can oligomerize, it is unable to transport pyruvate alone [26]. Many diseases are caused by dysregulation of the generation or utilization of the pyruvate node of metabolism and identification and characterization of the MPC1 and MPC2 have led to advances in treatments that target these proteins. Most notably is the dysregulation of the pyruvate node in cancer cells known as the ‘Warburg effect’, where large amounts of pyruvate are converted to lactate even when oxygen is present (aerobic glycolysis) [19].

Chapter 2 Materials and Methods

Table 2-1 Strains and Plasmids used in this study

Bacterial strain or Plasmid	**Relevant properties**	**Reference**
E. coli		
DC10B		
MC4100	[λΔ(SR)]	
S. aureus		
UAMS-1	clinical osteomyelitis isolate	[27]
KB1065	UAMS-1 *ΔcidA*	[28]
KB1060	UAMS-1 *ΔcidB*	[28]
KB1058	UAMS-1 ΔcidC::erm/ Em^R	[29]
KB1063	UAMS-1 *ΔlrgA*	These studies
KB1061	UAMS-1 *ΔlrgB*	These studies
KB1064	UAMS-1 *ΔlrgAB*	These studies
UAMS-1-*ccpA*	UAMS-1 *ΔccpA*::*tetL*/ Tet^R	[30]
JE2	USA300 LAC cured of all plasmids	[31]
NE1438	JE2 *lrgA*::ΦNE	[31]
NE1801	JE2 *0841*::ΦNE	[31]
NE1884	JE2 *0844*::ΦNE	[31]

NE626	JE2 *sdhA*::ΦNE	[31]
NE92	JE2 *qox*::ΦNE	[31]
NE117	JE2 *cydA*::ΦNE	[31]
NE592	JE2 *atpA*::ΦNE	[31]
Plasmids		
pLI50	*E. coli- S. aureus* shuttle vector	[32]
pEM80	*lrgAB* promoter::sGFP/ Cm^r	[33]
pJE30	pLI50::*lrgAB* (under control of its native promoter)	These studies
pJE31	pLI50::*lrgA* (under control of its native promoter)	These studies
pJE32	pLI50::*lrgB* (under control of its native promoter)	These studies
pSC8	pS-FX/R+ with *cidA*	These studies
pSC9	pS-FX/R- with *cidA*	These studies
pSC20	pS-FX/R+ with *lrgA*	These studies
pSC21	pS-FX/R- with *lrgA*	These studies

Table 2-2 Primers used in this study

Primer name	**Sequence (5'-3')**
lrgAB_comp_F	CCACGAATTCAAACGTATTGAACAAGCAGTC
lrgA_comp_R	TTTTGGATCCGGTGTGTTTAGTGCTAAGTGG
lrgAB_comp_R	TTTTGGATCCGCTATTATCTTGCTTAGGTTTTTCG
JBLRGA1.2	CCGAATTCAGAATCTGGAACTGGTAGTGC
JBLRGA2	CCCTCGAGTTACACGACCATTGCCTCCTACGTTTG
JBLRGA3	CCCTCGAGCCAGCCGGTATCTCAGTTGTTAACTC
JBLRGA4	GGCTGCAGCGTCTATATCCCAGTTATAAACCGGAG
JBLRGA5	GGTGTCAAGATGCAAGTTGGACGTTC
JBLRGB1	CCGAATTCGCGACTAAAGCCAAAGATGATAATAGCGCA
JBLRGB1.2	CCCCGAATTCGCGACTAAAGCCAAAGATGATAATAGCGCA
JBLRGB2.2	CCCGGCTCGAGGTTAATCATGAGCTTGTGCCTCCTC
JBLRGB3	CCCTCGAGTAAAACGAAAAACCTAAGCAAGATAATAGC
JBLRGB4	GGCTGCAGCCTGCATCCACATCGTATGGCC
JBLRGB6	GGACTAGTCCCAGTTATAAACCGGAGTATAGACG

Bacterial strains, plasmids and growth conditions

The bacterial strains used for this study are listed in Table 2-1. For convenience, in this manuscript we have referred to MC4100 [λΔ(*SR*)] cells as Δ*SR* cells. Δ*SR* cell cultures were grown in LB medium supplemented with 100 µg/mL ampicillin. Lysis curves were obtained by measuring A_{550} after thermal induction at 42˚C. Briefly, cultures of Δ*SR* cells carrying pS105-derived plasmids were grown aerobically (250rpm) at 30°C until A_{550} ~ 0.3, followed by thermal induction for 20 minutes at 42°C. The cultures were then incubated at 37°C for 6 hours to observe lysis (OD_{550}) and viability (cfu/ml).

S. aureus strains were grown overnight in tryptic soy broth (TSB) medium (BD biosciences) at 37° C with aeration at 250 rpm. For growth curves the overnight cultures were pelleted and resuspended into chemically defined medium (CDM) that was prepared as previously described [34] with either pyruvate or glucose to a final concentration of 30 mM or 15 mM, respectively. Cultures were then inoculated to a final OD_{600} of 0.05 and growth was monitored by OD_{600} measurements taken every 30 minutes on a Tecan plate reader.

Membrane preparation and western blotting

Cultures of Δ*SR* cells transformed with pS-F-sam7/R^{-}, pS-F-miniBax/R^{-}, pS-F-cidA/R^{-}, or pS-F-lrgA/R^{-} plasmids were grown in 50ml LB supplemented with 100µg/ml ampicillin to A_{550} ~0.3 at 30° C, induced for 15 min at 42°C, and then grown at 37° C for two hours. At two hours, 50ml cultures were passed through EmulsiFlex-C5 three times at the pressure of 15,000 psi. The membranes were collected by ultracentrifugation at 100,000 g for 60 minutes at 4° C and resuspended in 200 µl of 1X PBS containing proteinase

inhibitor (Roche #11836170001). For western blotting, resuspended membrane fractions were mixed with 3X SDS sample buffer, subjected to SDS-PAGE, and analyzed by western blotting with an anti-Flag antibody (Sigma #F3165).

Western blot analysis and EGS/BMH-cross linking

For the cross-linking reactions, the final protein amount per reaction was normalized by the cell amount and assessed as total A_{550} units collected. Briefly, 100 μL of membrane fraction was incubated with or without crosslinker, BMH (0.2 mM), EGS (1mM), for 1 h at room temperature with gentle shaking. The reaction was stopped by the addition of DTT (50 mM) with incubation for another 15 min at room temperature. The membranes were recollected by ultracentrifugation as described above and solubilized in 100ul of lysis buffer at 4° C for 3-4 hours. The insoluble material was removed by centrifugation at 17,000*g* for 5 min at 4° C. The soluble fraction was mixed with 3× SDS sample buffer, subjected to SDS-PAGE, and analyzed by western blotting with an anti-Flag antibody.

Protein expression and purification

To purify the proteins from *E. coli*, the previously described plasmids pDR7 and pDR8, which are the *cidA* or *lrgA* gene, respectively, ligated into pET24b (Novagen) were transferred into *E. coli* strain C43, a mutant derivative of BL21 (DE3) [35]. *E. coli* BL21 cells containing plasmid were grown at 37˚ C (200rpm) in 2X TY medium supplemented with Kanamycin (0.1mg/ml). Culture OD_{600} was monitored until it reached OD600~3, then the cultures were cooled down to 27° C for an hour in the incubator and induced with 1mM

isopropyl β-D-1-thiogalactopyranoside (IPTG) for protein expression. Protein expression was continued until OD_{600} reached ~5.0 to 6.0 when *E. coli* cells were centrifuged in a Beckman S-5.1 rotor at 5000 rpm for 10 minutes at 4º C and stored at -20º C.

Frozen *E. coli* BL21 cells expressing CidA /LrgA protein were lysed by adding 0.1% Triton X-100, 0.8 M Urea, 0.25 mg/ml lysozyme and Pierce universal nuclease (Thermo Fisher Scientific) followed by stirring at room temperature for 1 hour. Total membrane solubilization was achieved by the addition of 1.75% empigen BB detergent (Sigma Aldrich) and further incubation at room temperature for 1 hour. Insoluble material was removed by centrifugation at 7500 g and 4º C for 1 hour. Protein purification was performed by using an AKTA Purifer 10 (GE Healthcare) system. First, the total cell solubilized material was loaded onto a 20 ml HisPrep FF 16/10 column (GE Healthcare) pre-equilibrated with 20 mM Tris, 0.7% Empigen, 3 M Urea, 500 mM NaCl and 60 mM Imidazole buffer, pH 8.0. The column was then washed with 200 ml of the same buffer followed by 20 mM Tris, 0.1% DDM and 60 mM Imidazole, pH 8.0. Second, CidA/LrgA was eluted from the Ni resin using 20 mM Tris, 0.1% DDM and 500 mM Imidazole, pH 8.0 and directly applied onto a 25 ml 200 increase 10/300 Superdex column (GE healthcare) for a second-step purification in 20 mM Tris, 0.1% DDM pH 8.0. Purified protein was stored at -20º C in the presence of 20% glycerol.

Membrane reconstitution

CidA/LrgA in n-Dodecyl β-D-maltoside (DDM) was reconstituted into a membrane system of phospholipid composition POPG/POPC = 7:3 by detergent dialysis. Lipids were dissolved in chloroform and stored at -20º C. Required aliquots were mixed and chloroform

was then removed under low vacuum followed by overnight lyophilization. The dried lipid mixtures were then dissolved in 20 mM Tris, 60 mM OG, pH 8.0 at a final concentration of 2.5 mg/ml and vortexed until clear. OG-solubilized lipids and CidA/LrgA were then combined and incubated at room temperature for 30 minutes. After incubation, the mixture was dialyzed using a 10 kDa cutoff membrane against 20 mM Tris, 50 mM NaCl, 2 mM EDTA for 24 hours. The amount of protein, if any that becomes embedded in the liposomes is dependent on the speed at which the detergent is removed from the mixture [36].

Transmission Electron Microscopy

Samples were incubated with 5 nm Ni-NTA-Nanogold (Nanoprobes, Yaphank, NY) to label CidA/LrgA for 30 minutes. 10 µL of the sample was then placed on thin holey carbon films grids and allowed to absorb for 2 minutes. The grids were then washed with 10 µL of deionized water twice and negatively stained with methylamine vanadate (Nanoprobes). Imaging was carried out with a Tecnai G2 transmission electron microscope (FEI) operated at 80 kV.

Carboxyfluorescein liposome leakage assay

The newly developed liposome leakage assay was based on the self-quenching property of carboxyfluorescein (CF, a negatively charged fluorescent dye). The POPG/POPC (7:3) lipids were dried and dissolved in 60 mM OG as described above in the dialysis-based membrane reconstitution method. The liposomes were combined with a small amount of DDM dissolved CidA/LrgA protein and the mixture was then directly injected with 50 mM CF (CF self-quenches at this concentration), 20 mM Tris, 50 mM

NaCl and 2 mM EDTA solution. The proteo-liposomes with detergent molecules were formed upon dilution since the detergent concentration was below critical micelle concentration (CMC, for CMC_{OG}= 15-17 mM, CMC_{DDM}~0.2 mM). The newly formed liposomes trap a small amount of 50 mM CF. Free dye and the proteoliposomes are separated by PD-10 columns and the collected liposomes are subjected to 10 ul of 10% Triton X-100 and water, respectively. Upon lysis by Triton X-100, the 50 mM CF entrapped inside the liposomes was immediately diluted and emitted stronger fluorescent signal. Fluorescent signal was measured by spectrometer at endpoint excitation wavelength 492 nm and emission wavelength 517 nm. The signal is calculated as: $\Delta FL = FL_{Triton\ X\text{-}100} - FL_{water.}$

ΔFL represents the difference in fluorescence signal, $FL_{Triton\ X\text{-}100}$ represents the signal obtained from Triton X-100 added liposomes (lysed) and Fl_{water} stands for water added liposomes (not lysed). A negative control was made by using plain DDM detergent without proteins. By comparing the ΔFL of CidA/LrgA proteo-liposome and the control liposome, the extent of leakage by membrane trapped protein is calculated.

Confocal imaging of liposomes

Protein embedded multilemilar liposomes were generated by electroformation and the protein stain NTA-Atto 647 N (Sigma-Aldrich) was used to stain the CidA/LrgA protein. 5(6)-Carboxyfluorescein (Acros Organics) was then added and the liposome leakage was imaged on a Zeiss 710 confocal scanning microscope fitted with an EC Plan-Neofluar 40X/1.30 oil (DIC) M27 objective. Carboxyfluorescein was excited with the

Argon 458/488/514nm laser while, the NTA-Atto 647 N was excited with the DPSS 561nm.

Generation of the *lrgA, lrgB and lrgAB* mutants and complement strains

The *lrgA* mutation in UAMS-1 was generated by allelic exchange as previously described, utilizing the temperature sensitive plasmid pCL52.2 [32]. First, ~1000 bp of the upstream region of *lrgA* was PCR amplified using primers JBLRGA1.2 and JBLRGA2. The pcr product was digested with EcoRI and XhoI, gel purified and ligated into EcoRI;XhoI digested, pCL52.2, the resulting plasmid was named, pJB27. Next, roughly 1000 bp of the downstream region of *lrgA* was pcr amplified using JBLRGA3 and JBLRGA4, the resulting PCR product was digested with PstI and XhoI and ligated into the PstI;XhoI digested pJB27, and this plasmid was named pJB30. To generate the *lrgB* mutant primers JBLRGB1 and JBLRGB4, that added EcoRI and PstI, were used to amplify the entire *lrgAB* operon along with ~500 bp upstream of the *lrgA* start codon and ~1000 bp downstream or the *lrgB* stop codon this fragment was cloned into pcr2.1, generating pJB2. To remove the XhoI site from pJB2 the plasmid was digested with XhoI, klenow treated and then self-ligated which generated plasmid pJB10. Primers JBLRGB2.2 and JBLRGB3 were used to add an XhoI site and amplify around pJB10 the product was then self-ligated with XhoI, resulting in the removal of *lrgB*. Finally, the HindIII and XbaI sites were used to move the fragment carrying ~941bp upstream of *lrgB* and 1023bp downstream of *lrgB* into pCL52.2 generating plasmid pJB14. Lastly, to generate the *lrgAB* mutant a 1042 bp region downstream of *lrgB* was amplified with JBLRGB3 and JBLRGB4 adding PstI sites which was then ligated to PstI digested pCL52.2 generating plasmid pJB4. The upstream region of *lrgA* was then amplified with JBLRGA1.2 and JBLRGA2 creating a ~1000 bp

fragment with EcoRI and XhoI that was ligated to similarly digested pJB4 creating plasmid pJB27. These plasmids were then electroporated into RN4220 and moved into UAMS-1 via ϕ11 mediated phage transduction [37]. Following plasmid confirmation, allelic exchange was carried out as previously described [38] and the mutations were confirmed by PCR amplification. Primers JBLRGA4 and JBLRGA5 were used to confirm the *lrgA* mutation, the *lrgB* mutant was confirmed with primers JBLRGA5 and JBLRGB6 and the *lrgAB* mutant confirmed with JBLRGB1.2 and JBLRGB4. All primers are listed in Table 2-2.

The *lrgA* complement plasmid was generated by PCR amplification of ~500 bp upstream of the *lrgA* start site and ending at the *lrgA* stop codon with primers lrgAB_comp_F and lrgA_comp_R that added an EcoRI and BamHI restriction sites to the product. The resulting 1003 bp product was digested and ligated into the EcoRI and BamHI digested pLI50 generating plasmid pJE31. The *lrgAB* and *lrgB* complement plasmid were generated with primers lrgAB_comp_F and lrgAB_comp_R, UAMS-1 wild-type DNA was used as the template for the *lrgAB* complement while, the *lrgA* mutant was utilized as the template for *lrgB*. The PCR fragments were then digested and ligated into the EcoRI/BamHI sites of pLI50 and named pJE30 and pJE32, respectively. The plasmids were then electroporated into RN4220 and moved into the appropriate isolate by ϕ11 mediated phage transduction.

Metabolite analysis

For growth and sampling for metabolite analysis, bacterial cultures were grown in CDM as mentioned above except they were inoculated into a flask. For aerated samples they were grown with a 1:10 volume to flask ratio at 37° C and shaking at 250 rpm. While,

microaerobic samples were grown with a 3:5 volume to flask ratio and the shaking was reduced to 50 rpm.

For the pyruvate analysis, 1 ml samples were taken every 2 hrs until 8 hrs of growth and then again at 24 hrs of growth. The bacteria were pelleted and 900 ul of supernatant was removed to a clean epi tube and samples were frozen at -20° C. The pyruvate assay was performed as previously described [39, 40]. Briefly, samples were diluted and added to a black 96-well plate with a clear bottom and brought to 50 ul total volume with the pyruvate assay buffer (100 mM potassium phosphate, 1 mM EDTA and 1 mM $MgCl_2$).Then 150 ul of the enzyme mix was added to each well and mixed by pipetting, the plate was incubated for 15 minutes at room temperature in the dark and then the OD_{570} was taken on a Tecan microplate reader. A standard curve from 0 mM to 10 mM was generated and used to calculate the amount of pyruvate per well.

The amount of extracellular acetate and lactate was calculated using the acetic acid test kit (R-biopharm #10148261035) or the D-Lactic acid/L-lactic acid kit (R-biopharm #11112821035) per the manufacturer's instructions but adjusted to be performed in a 96-well plate. Briefly, 10 ul of supernatant was added to the wells of a 96- well microtiter plate (Corning 3596) and followed by the addition of the master mix (313 ul for acetate and 216 for lactate) and then read at 340 nm following a 15 or 30 minute incubation, respectively, at room temperature.

Chapter 3 The *Staphylococcus aureus* CidA and LrgA proteins are functional holins

Introduction

The control of bacterial lysis induced by bacteriophage infection is a highly coordinated process that is both elegant and simplistic in nature. This precisely timed event is controlled primarily by two proteins: 1) a murein hydrolase (or endolysin) that specifically degrades the cell wall of the infected cell and 2) a small membrane-associated protein, termed a "holin", that controls the access or activity of the murein hydrolase to the peptidoglycan. The latter has the unique ability to function as a biological timer, delaying peptidoglycan degradation so that bacteriophage assembly can be completed before lysis ensues [41-44]. The holin, thus, functions as a master regulator of cell death and lysis akin to the regulatory control of programmed cell death (PCD) in more complex eukaryotic organisms [45, 46]. Surprisingly, the most well-studied form of PCD in these organisms (termed "apoptosis") is also controlled by small membrane-associated proteins (the Bcl-2 family) that target mitochondria [47, 48]. Indeed, studies revealed that these proteins functionally complement holin defective bacterial strains, inducing cell death and lysis [45]. These results led to the conclusion that members of the Bcl-2 family of proteins are functional holins [45] and that the processes underlying the control of apoptosis evolved from bacteria [46, 49].

Our understanding of bacterial PCD has also been shaped by the study of proteins proposed to possess holin-like activity, specifically through investigations of the *Staphylococcus aureus* CidA and LrgA proteins, which share many characteristics in

common with holins. These proteins are also small in size, they contain two or three transmembrane domains, and their C-terminal domain is highly charged while containing a polar N-terminus [50]. Besides these structural similarities, the CidA and LrgA proteins have also been shown to oligomerize into high-molecular-mass structures that are dependent on cysteine disulfide bonds similar to the S105 holin [35, 51]. Early investigations revealed that *cid* and *lrg* mutations caused alterations in murein hydrolase activity and autolysis, consistent with their structural similarities to holins [50, 52, 53]. These studies led to the hypothesis that the *cid*/*lrg* family of genes, which are well-conserved in bacteria, as well as in the Archea and plants, are important regulators of PCD [46, 54, 55]. Subsequently, the biological role of these genes was associated with biofilm development, a multicellular context in which PCD could provide a selectable benefit [54].

More recently, the genes encoded within the *cidABC* operon have been shown to play an important role in regulating cell death during overflow metabolism [30, 56]. The CidA and CidB proteins have opposing effects on CidC, a pyruvate:menaquinone oxidoreductase [57] that results in alterations in the extracellular acetate and acetoin levels [56]. It was hypothesized that *cidA* and *cidB* encode transport proteins involved in the secretion of these two metabolic byproducts [56]. Consistent with this was the finding that plant homologs of the *cidAB* and *lrgAB* genes (the *Arabidopsis thaliana* PLGG1 gene, also referred to as AtLrgB) are required for the transport of glycerate and glycolate, two small carbohydrate intermediates important in the Calvin cycle of photosynthesis [58]. In addition, it has been shown that the *lrgAB* operons of *Bacillus subtilis* and *Streptococcus mutans* are required for pyruvate transport [59-62]. The *B. subtilis lrgAB* operon is induced as the amount of extracellular pyruvate increases and mutations within the operon exhibit

growth defects when grown on media with pyruvate as primary carbon source. Also, the *B. subtilis lrgAB* operon appears to regulate the intracellular levels of pyruvate as it can also act as an exporter under conditions that promote the accumulation of this metabolite in the cytoplasm [59]. Similarly, although *S. mutans* is unable to grow in media with pyruvate as the sole carbon source, introduction of a *lrgAB* mutation resulted in the inability to import pyruvate once the cultures reached stationary phase when other primary carbon sources have been consumed [61].

In the current study, we use genetic and biophysical approaches to demonstrate that both CidA and LrgA are functional holins. In addition, we demonstrate that the *lrgAB* operon is involved in pyruvate import under low oxygen conditions, in contrast to the *cidABC* operon, which was previously shown to affect the export of acetate and acetoin. These studies suggest that the *cidABC* and *lrgAB* operons play a dual role, one as an effector of cell death and the other as transporters of metabolic byproducts of carbohydrate metabolism.

Results

Functional complementation using cidA and lrgA

Although holins are manifested in a variety of different forms, confirmation of holin function can be achieved using the *E. coli* ΔSR/pS105 holin-expression system developed by Smith et al. [63]. The plasmid, pS105, contains a "λ-lysis cassette" (Figure 3-1), encoding a holin (S105), R protein (an endolysin) and two accessory proteins, Rz and Rz1. These proteins are products of the λ genes transcribed from the promoter, $P_{R'}$. The *E. coli* ΔSR cells maintain a thermally inducible λ prophage that is lysis defective due to deletion of both *S* (S105) and *R* genes. Following thermal induction, the prophage supplies the late

gene activator Q required for transactivation of the pR′ promoter on pS105 and, thus, allows expression of genes within the lysis cassette. The coupled expression of the S105 holin and endolysin following thermal induction causes lysis of the *E. coli* ΔSR cells, which can be measured spectrophotometrically. Given that lysis is holin dependent, the ability of a heterologous gene to replace the lysis-inducing capacity of S105, therefore, provides a simple way to assess whether or not this gene encodes a functional holin.

To determine if CidA and/or LrgA exhibit holin-like activity, we constructed derivatives of pS105 (pS-F-CidA/R^+ and pS-F-LrgA/R^+), wherein the gene encoding FLAG-tagged CidA or LrgA replaced the *S* gene encoding the S105 holin (Figure 3-1A), and transferred these plasmids into *E. coli* ΔSR cells. Upon thermal induction, the *E. coli* ΔSR cells underwent a steady rate of cell lysis compared to the holin negative control (*sam7*) that lasted over a period of six hours (Figure 3-2A and Figure 3-3A). To test whether the observed lysis was dependent on endolysin (R), we used an endolysin negative construct, pS-F-CidA/R^- or pS-F-LrgA/R^- (Figure 3-1B), with a stop codon introduced in the *R* gene. As shown in Figure 3-2A and Figure 3-3A, the null mutation in *R* abolished CidA and LrgA-dependent cell lysis demonstrating that lysis was not the result of a general toxicity effect of CidA and LrgA. Importantly, cell viabilities decreased upon expression of CidA or LrgA regardless of endolysin activity (Figure 3-2B and Figure 3-3B), indicating the loss of membrane integrity following expression as was previously reported for holins [41]. As a positive control, we utilized *E. coli* ΔSR cells containing the plasmid pS-F-minibax/R^+ that was previously shown to induce lysis in this system [45].

To test if CidA and LrgA-dependent cell lysis correlated with membrane localization and oligomerization, we determined the level of *cidA* and *lrgA* expression and

localization by probing ΔSR cell membrane fractions collected at different time-points after thermal induction with anti-FLAG antibodies (Figure 3-2C and Figure 3-3C). The extent of oligomerization was determined by cross-linking CidA or LrgA complexes with either ethylene glycol bis(succinimidyl succinate) (EGS) or bismaleimidohexane (BMH), respectively, prior to SDS-PAGE analysis and western blotting using anti-FLAG antibodies. To achieve maximum signal intensity, both membrane localization and EGS/BMH cross-linking studies were carried out in the R^- (endolysin negative) background. Upon thermal induction, we observed a time-dependent accumulation of CidA or LrgA within the *E. coli* ΔSR cytoplasmic membrane (Figure 3-2C and Figure 3-3C). Furthermore, like bacteriophage holins, cross-linking CidA with EGS revealed the presence of homodimers including higher order oligomers (Figure 3-2D). While the presence of the higher order LrgA oligomers were not observed, the LrgA monomer was much fainter in the presence of the crosslinker suggesting that oligomerization may be occurring but distinct oligomeric bands were too scarce to be detectable (Figure 3-3D). Collectively these data suggest that cell lysis resulting from heterologous expression of CidA or LrgA in *E. coli* ΔSR cells is associated with the membrane localization and oligomerization of these proteins, likely resulting in the formation of pores large enough to allow for the passage of the ~18 kDa *R*-encoded endolysin.

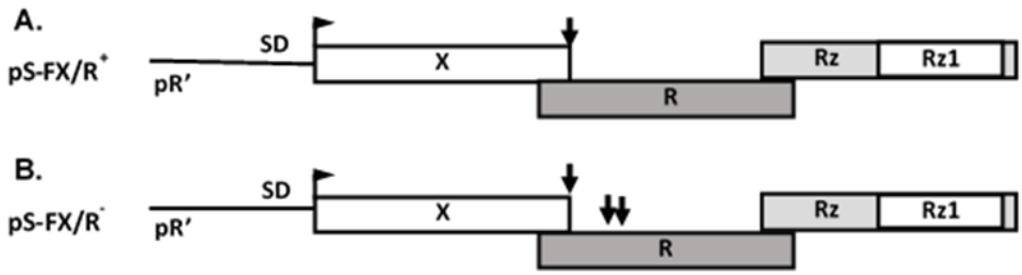

Figure 3-1 Schematic representation of bacteriophage lambda lysis cassette.
The Flag-tagged S105 holin was replaced with either *cidA* or *lrgA* in (A) pS-FX/R+ plasmid that expresses endolysin or in (B) pS-FX/R- that has a stop codon (arrows) introduced so no functional endolysin is produced. pR', λ late promoter; SD, Shine-Dalgarno sequence; X, S105; R, endolysin and accessory proteins Rz and Rz1.

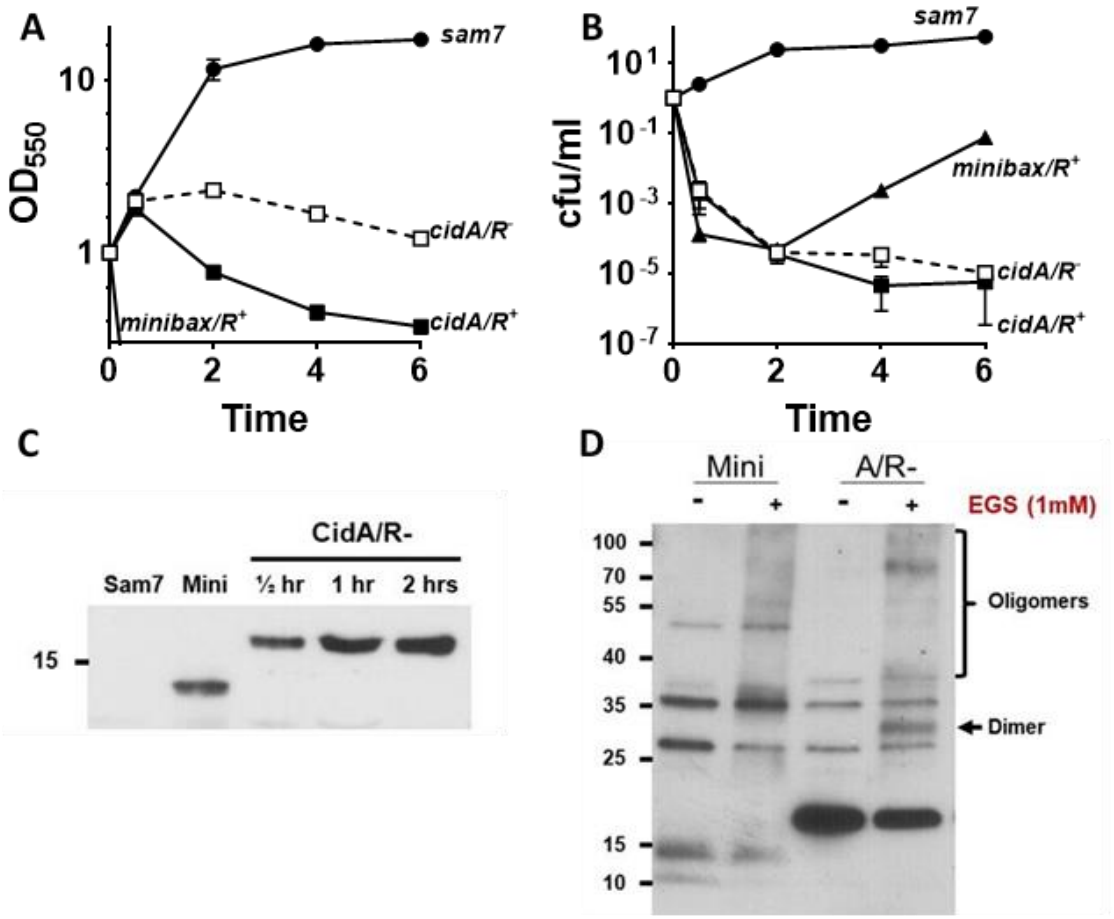

Figure 3-2 CidA protein exhibits holin-like properties.
(A) ΔSR cell lysis and (B) cell viability was monitored after expression of pS-F-CidA/R+ and pS-F-CidA/R-. pS-sam7/R+ and pS-F-minibax/R- are used as negative and positive controls. (C) Localization of CidA protein to the ΔSR cell membranes was detected by western blot using monoclonal α–Flag antibodies. pS-sam7/R+ and pS-F-minibax/R- are used as negative and positive controls. (D) CidA Oligomerization in ΔSR cell membranes was determined by amine reactive cross linker, EGS (1 mM). The protein concentration was adjusted by normalizing the cell amount and assessed as total OD_{550} units collected. Membrane preparations were separated on a 10% denaturing polyacrylamide gel and stained using monoclonal α–Flag antibodies. The experiment was repeated three times and a representative gel image is shown. Images are courtesy of Sujata Chaudhari.

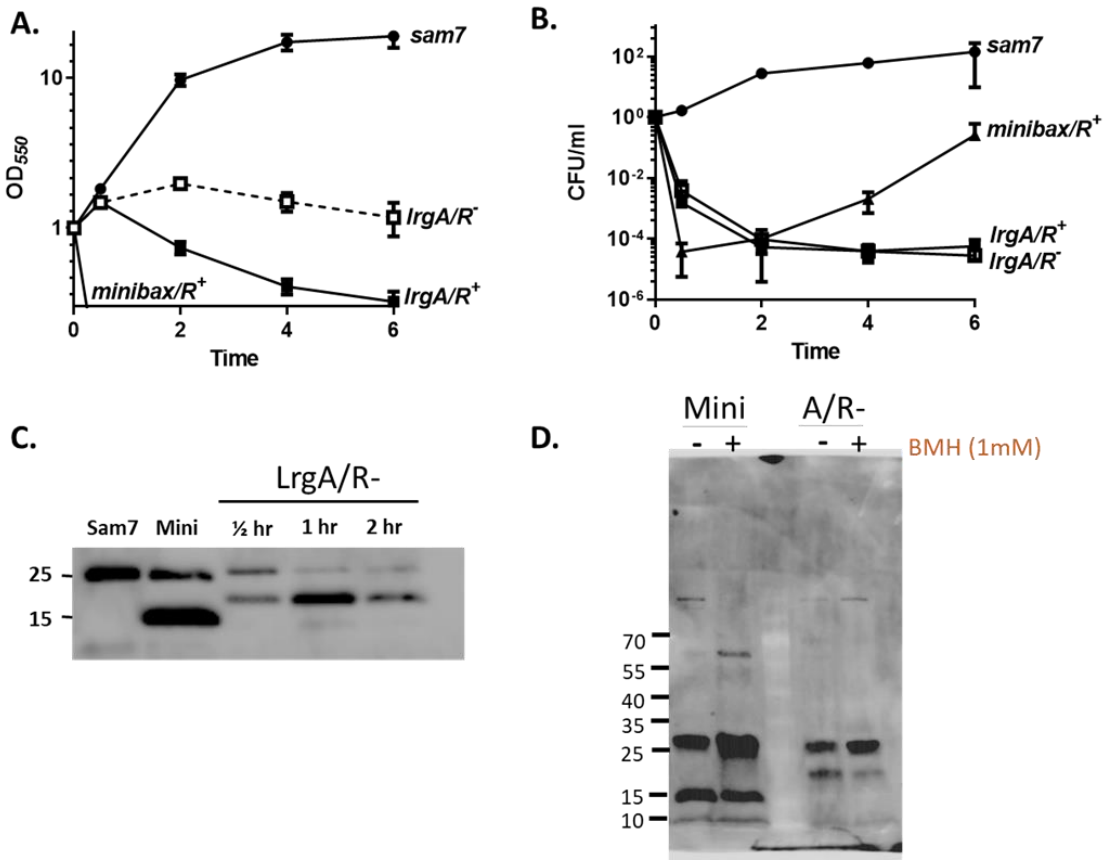

Figure 3-3 LrgA protein exhibits holin-like properties.
(A) ΔSR cell lysis and (B) cell viability was monitored after expression of pS-F-LrgA/R+ and pS-F-LrgA/R-. pS-sam7/R+ and pS-F-minibax/R- are used as negative and positive controls. (C) Localization of LrgA protein to the ΔSR cell membranes was detected by western blot using monoclonal α–Flag antibodies. pS-sam7/R+ and pS-F-minibax/R- are used as negative and positive controls. (D) LrgA Oligomerization in ΔSR cell membranes was determined by amine reactive cross linker, BMH (1 mM). The protein concentration was adjusted by normalizing the cell amount and assessed as total OD_{550} units collected. Membrane preparations were separated on a 10% denaturing polyacrylamide gel and stained using monoclonal α–Flag antibodies. The experiment was repeated three times and a representative gel image is shown. Panel C and D images are courtesy of Janani Prahlad.

CidA and LrgA form pores within artificial cell membranes

To provide direct evidence of the ability of CidA and/or LrgA to form a pore, we developed an *in vitro* protein-induced leakage assay using synthetic vesicles. We initially reconstituted recombinant CidA or LrgA fused to a C-terminal histidine-tag in a mixture of POPG/POPC lipids (7:3) by detergent dialysis as described in the Materials and Methods. The localization of the CidA-His or LrgA-His proteins within artificial membrane vesicles was assessed using 5 nm Ni^{2+}-gold nanoparticles that specifically bound to the His-tag. TEM analysis confirmed the incorporation of CidA-His or LrgA-His within the lipid membranes of artificial vesicles (data not shown). To determine whether CidA-His and LrgA-His formed functional pores, we loaded the protein containing vesicles with carboxyfluorescein (CF; ~376 Da) and assessed dye leakage from the interior of the vesicle. We used vesicles containing influenza M2, an ion channel transmembrane peptide as a negative control for our experiments. Influenza M2, only allows the passage of protons and not the large sized molecules such as CF even when added at high concentrations (data not shown). While CidA-His and LrgA-His both resulted in the leakage of the CF in a concentration-dependent manner, the amount of CidA-His necessary for leakage was much lower (Figure 3-4A). As a way to visualize the leakage of CF, we performed confocal imaging of these vesicles preparations where the dye was added externally to the vesicles containing either CidA-His or LrgA-His. The externally added CF dye entered only those vesicles that stained positive for the presence of CidA or LrgA membrane proteins (Figure 3-4B-C). Overall, 85% of the CidA-His containing vesicles and 72% of LrgA-His positive vesicles facilitated entry of the CF dye. In contrast, none of the vesicles lacking CidA-His or LrgA-His in their membranes allowed leakage of the CF dye. Based on these results, we

conclude that both CidA and LrgA promote pore formation within artificial membranes in a concentration-dependent manner.

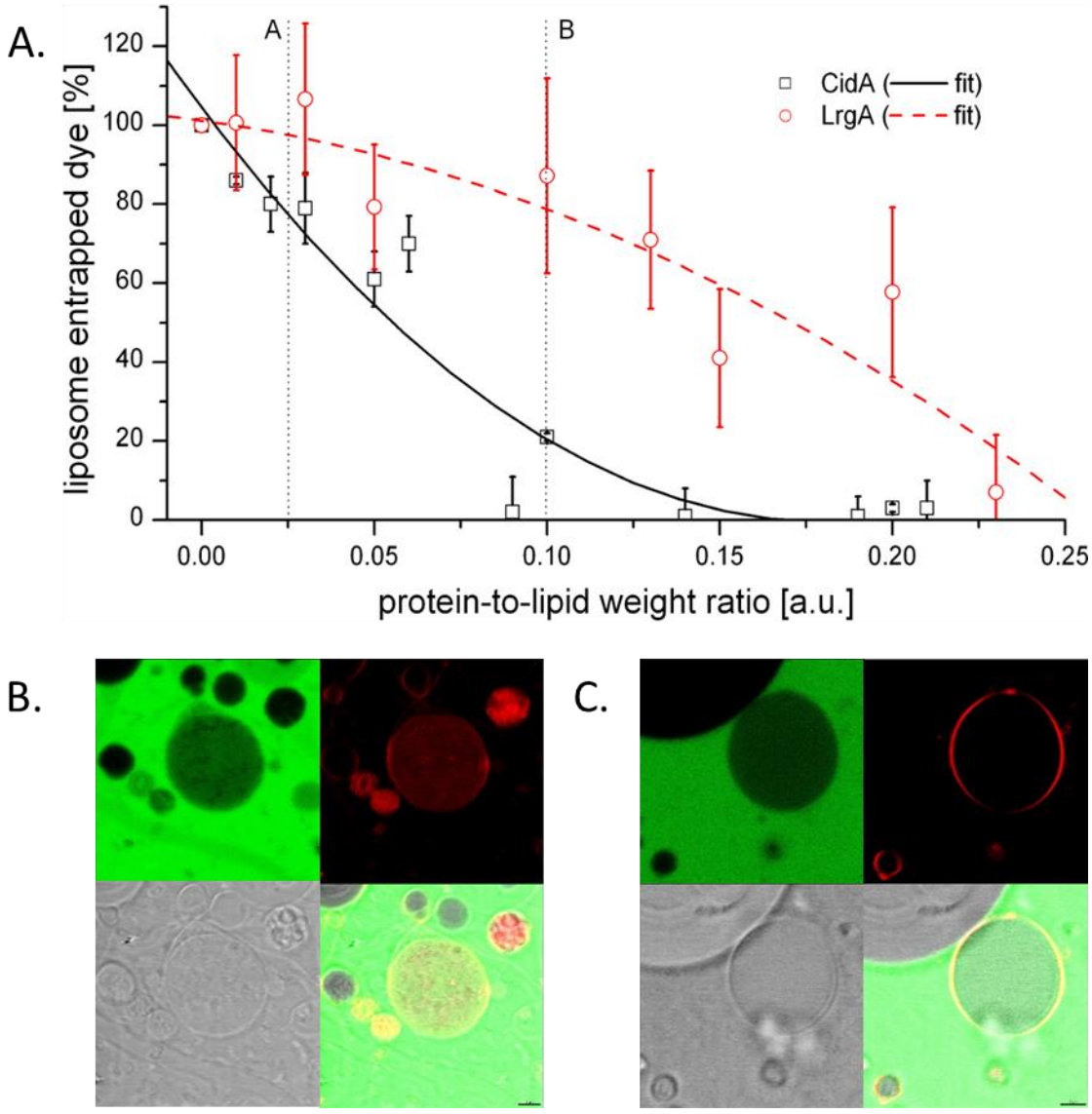

Figure 3-4 Liposome leakage assay of carboxfluorescein in the presence of CidA and LrgA. Liposomes are mixed with CidA or LrgA that are dissolved in DDM and then injected into 50 mM CF, 20 mM Tris, 50 mM NaCl and 2 mM EDTA solution. As the detergent levels drop the proteo-liposomes are formed and the newly formed liposomes trap the dye. Free dye is removed by separation on a PD-10 column and the collected liposomes are subjected to 10% Triton X-100 which causes lysis and the amount of entrapped dye is measured in a spectrometer (A). Liposomes are prepared with either CidA (B) or LrgA (C) and then atto dye (protein stain) as well as CF is added and imaged on a confocal microscope. Images are courtesy of Xinyan Zhang.

The lrgAB operon is required for pyruvate utilization under microaerobic conditions

In light of our previous report that the *cidABC* operon affects export of acetate/acetoin [56], combined with several studies demonstrating a role for *lrgAB* in pyruvate transport in other bacterial species [59-61], a *lrgA* clean deletion mutation was generated and growth was monitored in chemically defined media (CDM) containing either 15 mM glucose or 30 mM pyruvate. As shown in Figure 3-5, no growth defect was observed when the *lrgA* mutant was grown aerobically with either glucose or pyruvate (Figure 3-5B and D). However, when this mutant was grown with pyruvate as the sole carbon source under microaerobic conditions the *lrgA* mutant exhibited a dramatic growth defect (Figure 3-5A) that was not observed when glucose was provided as the sole carbon source (Figure 3-5C). In addition, the *lrgA* mutation resulted in an even more dramatic growth defect under anaerobic conditions with pyruvate as the primary carbon source (data not shown). Importantly, expression of *lrgA* from a plasmid from its native promoter restored growth of the mutant to wild type levels (Figure 3-5A), confirming the role of this gene under these conditions. To determine if this is a pyruvate-specific phenotype, growth of the *lrgA* mutant was assessed in the presence of other carbon sources (glycerol, fructose, malate, lactate, acetate and succinate) under aerobic and microaerobic conditions. As shown in Figure 3-6, although each carbon source supported different growth rates, the *lrgA* mutation did not alter the growth observed in the presence of these carbon sources. In contrast, the *cidABC* operon, which was previously shown to affect acetate and acetoin excretion [56], appears not to support pyruvate transport as mutations within these genes had no effect on growth using pyruvate as a carbon source (Figure 3-7).

The *lrg* operon consists of two co-transcribed genes, *lrgA* and *lrgB* [64]. While expression of LrgA alone has the ability oligomerize within the cytoplasmic membrane, cause death and lysis in the bacteriophage model, and form pores, it is likely that this protein functions in the context of LrgB. Thus, we speculated that disruptions of *lrgB* would also affect growth in the presence of pyruvate. To test this, mutations in *lrgB* and *lrgAB* were generated and their growth was assessed either during microaerobic or aerobic growth in CDM with pyruvate as the sole carbon source. As can be seen in Figure 3-8A, the *lrgA*, *lrgB* and *lrgAB* mutants demonstrated a similar growth defect when grown under microaerobic conditions suggesting that these isolates are unable to use pyruvate to support growth. The growth defects of the individual mutants can be complemented by expression of the corresponding gene from a plasmid (Figure 3-8B and C). However, plasmids carrying either *lrgA* or *lrgB* alone were unable to restore the growth of the *lrgAB* mutant suggesting that both LrgA and LrgB are necessary for the utilization of pyruvate when grown under microaerobic conditions.

To assess whether the defect in growth of the *lrgA* mutant in the presence of pyruvate as the sole carbon source was due to its inability to metabolize pyruvate, the amount of pyruvate remaining in the media after growth was measured for the wild type, *lrgA* mutant, and complemented strains. As shown in Figure 3-9A, growth of the wild-type and complemented strains under microaerobic conditions resulted in the removal of nearly all the pyruvate from the medium by 6 hr post inoculation, whereas the *lrgA* mutant was unable to remove any pyruvate even after 24 hr of growth. In agreement with the reduced consumption of pyruvate from the media, the *lrgA* mutant also exhibited a dramatic decrease in the amount of lactate and acetate generated during microaerobic growth in the

presence of pyruvate compared with the wild-type and complemented strains (Figure 3-9A). Consistent with the lack of an effect of the *lrgA* mutation on pyruvate uptake when grown aerobically or with glucose as the primary carbon source, the *lrgA* mutant did not exhibit any differences in the accumulation of lactate and acetate under these conditions compared with the wild-type and complemented strains (Figure 3-9B).

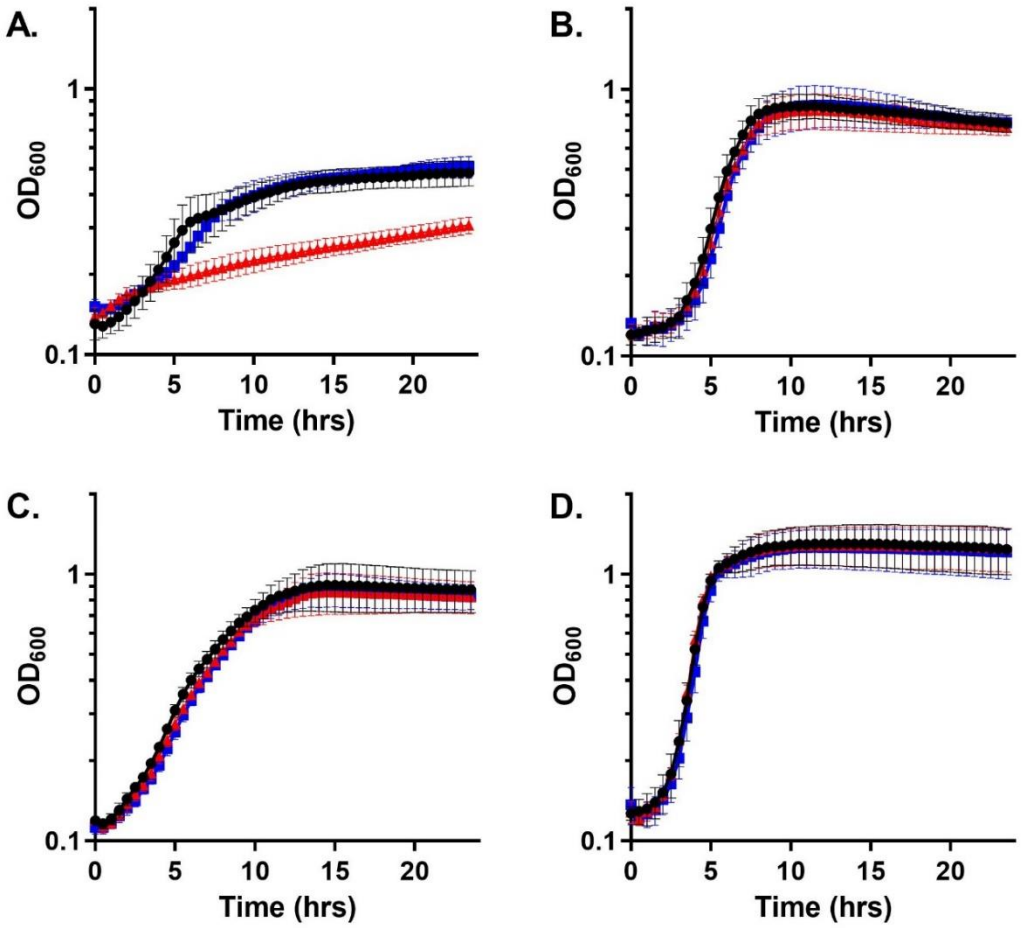

Figure 3-5 *S. aureus lrgA* is necessary for microaerobic growth with pyruvate as the sole carbon source.
Growth curves of *S. aureus* UAMS-1 (black circles), UAMS-1 *ΔlrgA* (red triangles), and UAMS-1 *ΔlrgA* with pJE31 (blue diamonds) in (A) CDM with 30 mM sodium pyruvate covered with oil, (B) CDM with 30 mM sodium pyruvate, (C) CDM with 15 mM glucose covered with oil, and (D) CDM with 15 mM glucose.

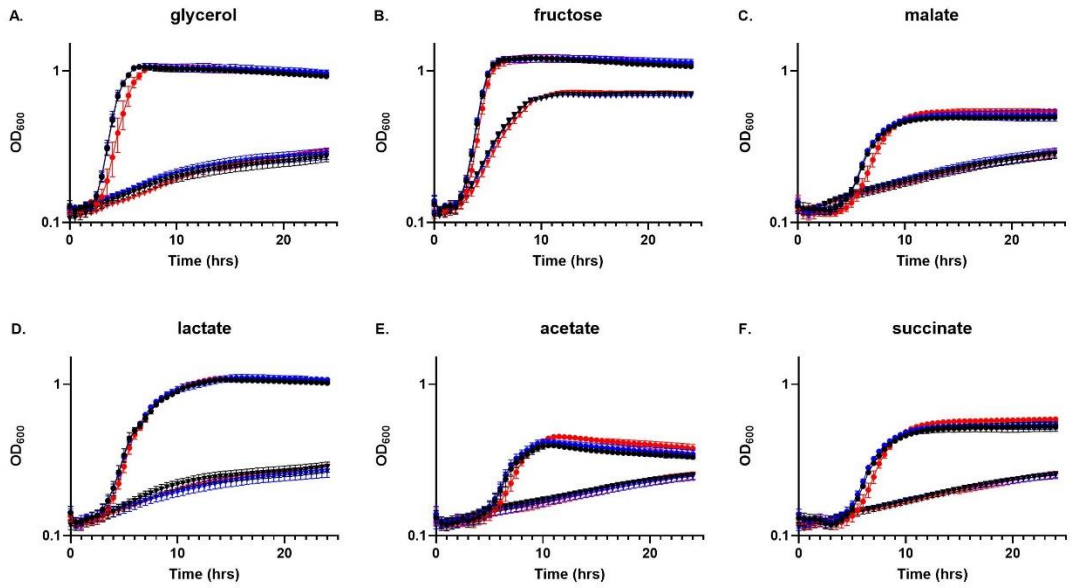

Figure 3-6 Aerobic (circles) and microaerobic (triangles) growth curves on different carbon sources.
UAMS-1 (black), UAMS-1 *ΔlrgA* (blue) or UAMS-1 *ΔlrgA* with pJE31 (red) grown on glycerol (A), fructose (B), malate (C), lactate (D), acetate (E), or succinate (F).

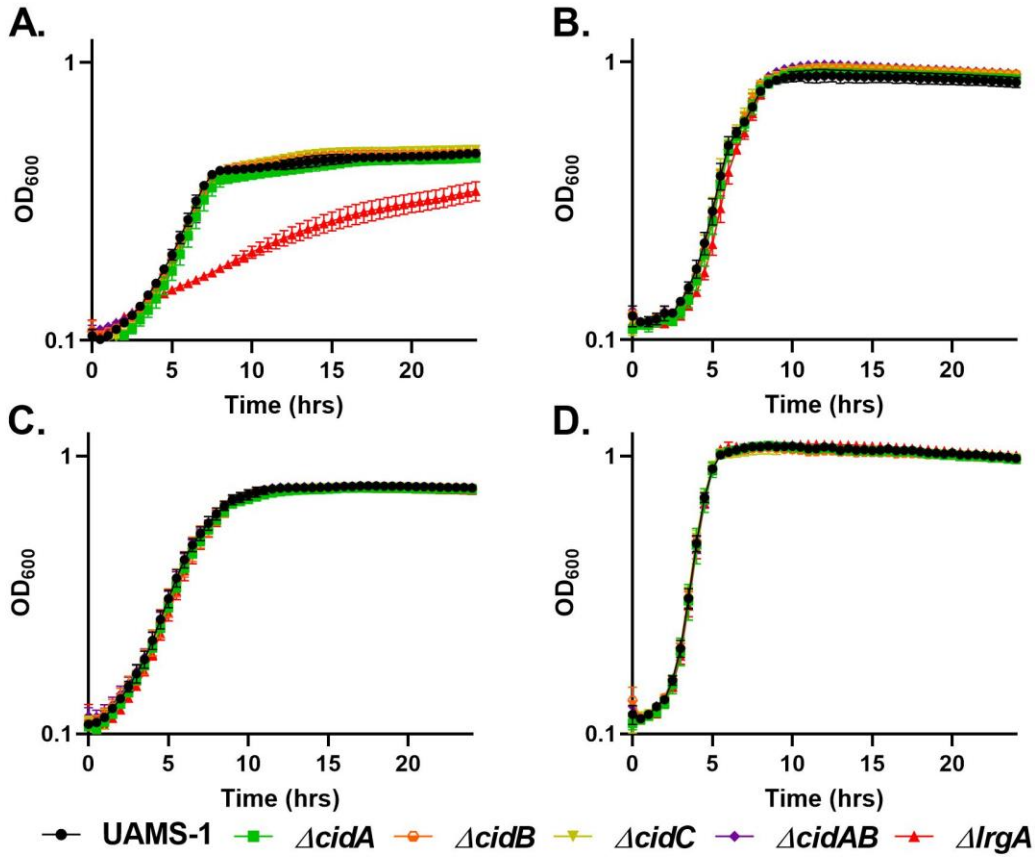

Figure 3-7 *S. aureus cid* operon is not required for microaerobic growth with pyruvate as the sole carbon source.
Growth curves of *S. aureus* UAMS-1 (black circles), UAMS-1 *ΔcidA* (green squares), and UAMS-1 *ΔcidB* (orange circles), UAMS-1 *ΔcidC* (yellow upside down triangles), UAMS-1 *ΔcidAB* (purple diamonds) and UAMS-1 *ΔlrgA* (red triangles) in (A) CDM with 30 mM sodium pyruvate covered with oil, (B) CDM with 30 mM sodium pyruvate, (C) CDM with 15 mM glucose covered with oil, and (D) CDM with 15 mM glucose. The UAMS-1 *ΔlrgA* was included as a control during all experiments with the *cid* mutants. All experiments were performed three times with triplicate technical replicates on each run.

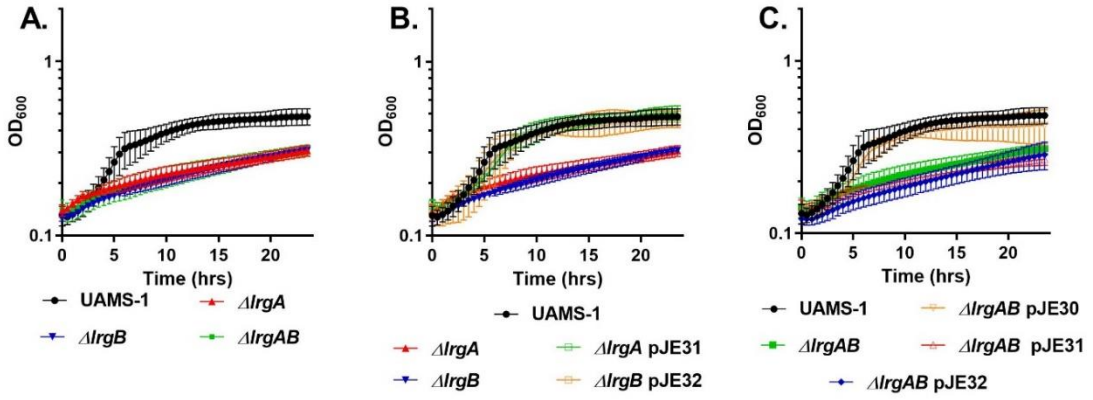

Figure 3-8 Both *lrgA* and *lrgB* are necessary for microaerobic growth with pyruvate as the sole carbon source.
Microaerobic growth curves in CDM with 30 mM pyruvate of *S. aureus* (A) UAMS-1, UAMS-1 *ΔlrgA*, UAMS-1 *ΔlrgB*, and UAMS-1 *ΔlrgAB*, (B) UAMS-1, UAMS-1 *ΔlrgA*, UAMS-1 *ΔlrgB* and complement strains UAMS-1 *ΔlrgA* with pJE31 and UAMS-1 *ΔlrgB* with pJE32 (C) UAMS-1, UAMS-1 *ΔlrgAB*, and complement strains of UAMS-1 *ΔlrgAB* carrying either pJE30 (*lrgAB*), pJE31 (*lrgA*) or pJE32 (*lrgB*).

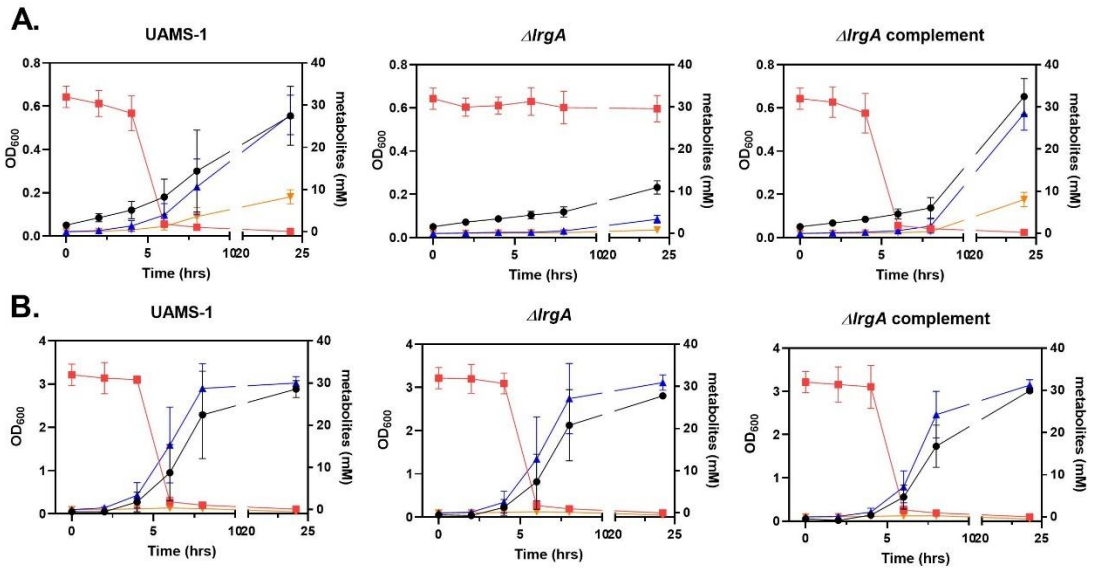

Figure 3-9 *S. aureus lrgA* is required for pyruvate removal from the media.
OD_{600} (black circles), extracellular pyruvate (red squares), acetate (blue triangles) and lactate (orange upside down triangles) were measured at 0, 2, 4, 6, 8 and 24 hrs for UAMS-1, UAMS-1 *ΔlrgA* and UAMS-1 *ΔlrgA* with pJE31 that were grown in CDM with 30 mM sodium pyruvate during either (A) microaerobic growth or (B) aerobic. Error bars represent the standard deviation from three independent experiments each with triplicate technical replicates.

Microaerobic growth with pyruvate induces lrgAB expression

The LytSR two-component regulatory system is necessary for induction of *lrgAB* expression upon disruption of the proton motive force and weak acid stress [65, 66]. Recent studies have also shown that pyruvate is also a potent inducer of *lrgAB* expression. To determine if pyruvate also stimulates *S. aureus lrgAB* expression, a *lrgAB* reporter fusion plasmid, pEM80 [33], was generated and monitored under microaerobic conditions in the presence of pyruvate. As shown in Figure 3-10, there was a 13-fold increase in GFP produced by the wild-type strain grown in the presence of pyruvate when compared to cells aerobically grown in the presence of glucose. Although the induction of *lrgAB* expression by pyruvate was shown to be *lytSR* dependent, some pyruvate-dependent induction was observed, this difference was found not to be statistically significant. These results demonstrate that *S. aureus lrgAB* expression is induced in a *lytSR*-dependent manner by growth in the presence of pyruvate.

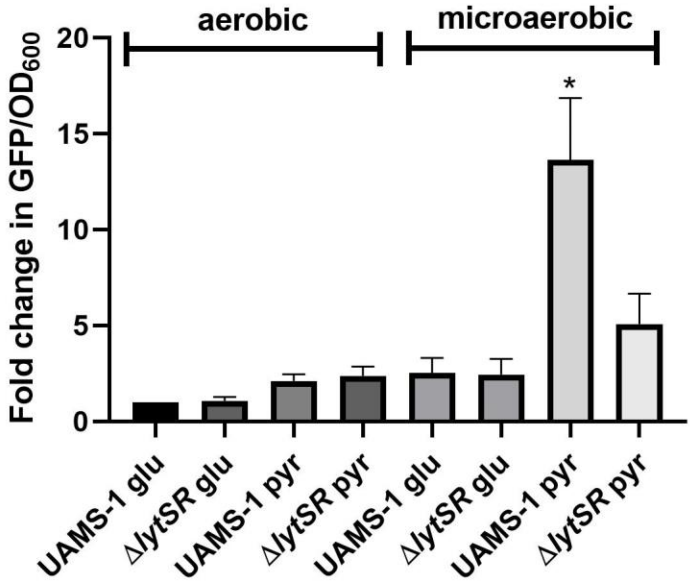

Figure 3-10 The *lrg* operon is optimally induced when grown under microaerobic conditions with pyruvate as primary carbon source.
S. aureus UAMS-1 with pEM80 is grown in CDM supplemented with either 15 mM glucose or 30 mM pyruvate and with high aeration or under microaerobic conditions. After 6 hrs of growth GFP is read on a Tecan M200 pro microplate reader with excitation at 488 nm and emission collected between 520-560 nm.

Discussion

The results presented in this report demonstrate that the *S. aureus cidA* and *lrgA* genes encode holins that are involved in the transport of pyruvate into the cell. Although their structural characteristics and impact on cell death and lysis have previously led us to speculate about their holin-like functions [67-69], the use of the "lysis cassette" system developed by Smith et al. [63] demonstrates, for the first time, that *cidA* and *lrgA* can support *E. coli* cell lysis (Figure 3-2A and Figure 3-3A) and, therefore, encode functional holins. These results also suggest that the *cidA* and *lrgA* gene products generate pores large enough for the release of the ~18 kDa endolysin [70, 71]. Based on our knowledge of how holins form pores [42, 63, 72, 73], we speculate that the *cidA*- and *lrgA*-encoded holins mediate import and export and have no selectivity for different molecules below a certain size. However, it is important to keep in mind that *cidA* and *lrgA* were expressed in the absence of their natural partners, *cidB* and *lrgB,* and are, therefore, likely functioning out of context of their normal molecular environment. In agreement with this, plasmids carrying either *lrgA* or *lrgB* alone were unable to complement the *lrgAB* mutant during microaerobic growth with pyruvate as the sole carbon source, while a plasmid carrying the entire *lrgAB* operon could, suggesting that both components of the operon are necessary under these conditions. Based on these results, we speculate that LrgA and LrgB form a complex within the membrane that functions in the capacity of a pyruvate transporter, and that LrgB provides specificity for pyruvate.

More than 150 holin genes have been identified and they encode one of the most diverse classes of genes with a common function [74]. Although there are a few exceptions, holins are characterized by their relatively small size, multiple transmembrane domains,

hydrophobicity, and their ability to oligomerize within the cytoplasmic membrane. Currently, there are two models of holin function, the canonical holin-endolysin and the pinhole-"SAR" endolysin system, both result in a precisely timed lysis of the cell by allowing an enzyme with muralytic activity to gain access to the peptidoglycan. The canonical holin-endolysin system generates pores in the membrane that are non-specific and are variable in size with an average hole size of roughly 340 nm +/- 35 [72], while the SAR endolysin model generates small 2 nm channels. Both systems cause the collapse of the proton motive force (PMF) allowing for either the release of cytosolic endolysin or for a membrane-embedded SAR endolysin to fold into an active conformation [75]. Given the size of the endolysin released by the lysis cassette used in this study, we speculate that CidA and LrgA function in a manner similar to the canonical holin-endolysin system.

A fundamental hypothesis driving our research on the *cidABC* and *lrgAB* operons is that they are important regulators of bacterial PCD and that this mechanism is fundamentally conserved in a wide variety of organisms spanning multiple Kingdoms of life. Using a similar "lysis cassette" approach that is described here, we reported that Bax and Bak, the two primary effectors of apoptosis, are functional holins [45]. Importantly, ten regulatory Bcl-2 proteins (similar to Bax and Bak, but playing auxiliary roles) expressed in the S105 holin system did not induce lysis, revealing a good correlation between Bcl-2 protein function and holin activity. One important aspect of holins is that despite the vast variations in the holin structure and differences in the mode of action of lysis, the end result is death and lysis of the bacterial cells [42, 74]. Thus, we used the lysis cassette system (Figure 3-1) to examine the ability of CidA and LrgA to support cell lysis. As shown in Figure 3-2 and Figure 3-3, both of these proteins supported robust cell lysis,

suggestive of lysis activity. As with other holins tested in this system, lysis was dependent on the presence of endolysin as the drop in optical density was not observed in strains lacking the R gene. In contrast, the viability loss observed was not R dependent, indicating that the integrity of the membrane was compromised by the expression of these proteins. Also, similar to holins, oligomers of CidA and LrgA were detectable in the membrane fractions of the R^- strains. Finally, the hole forming potential of CidA and LrgA was confirmed using liposomes reconstituted with purified CidA and LrgA, which induced leakage of carboxyfluorecein (Figure 3-4). While both CidA and LrgA induced carboxyfluoroscein leakage, CidA did so at much lower protein-to-lipid ratio than LrgA (Figure 3-4A), suggesting that its ability to form holes is more efficient.

Although our work on the CidA and LrgA proteins has been focused on their roles in bacterial PCD, it has become increasingly clear that they also serve as transporters of the by-products of carbohydrate metabolism [56, 76]. The first evidence of this was the observation that the *cidABC* operon is important for regulating bacterial cell death during overflow metabolism. Specifically, when excess glucose is present the *cidA* and *cidB* mutants exhibited opposing roles in the excretion of acetate and acetoin [56], the former likely due to the interaction of *cidA* or *cidB* with *cidC,* a pyruvate:menaquinone oxidoreductase that uses pyruvate as its substrate to generate acetate [57]. More recently, several studies have demonstrated the role of *lrgAB* homologs in the transport of pyruvate [59-61]. In *B. subtilis*, disruption of the *lrgAB* homologs (designated *ysbAB*) caused a significant growth defect when grown in LB media with pyruvate as the primary carbon source [59]. Similarly, the *S. mutans lrgAB* operon also appears to play a role in pyruvate import. Although *S. mutans* is unable to grow with pyruvate as the sole carbon source, a

lrgAB mutant was defective in pyruvate consumption upon entry into stationary phase [61]. Interestingly, the plant *lrgAB* homolog, *PLGG1*, has been shown to be important modulator of cell death [77], as well as in the transport of glycerate and glycolate during photorespiration [58].

To determine the potential role of the *S. aureus lrgAB* operon in pyruvate transport, we first examined the effect of a *lrgA* mutation on growth in the presence of this metabolite. Consistent with previous reports of metabolite transport, the *lrgA* mutant exhibited a growth defect when grown under microaerobic conditions on pyruvate. In addition, the *lrgA* mutant was unable to remove the pyruvate from the media during microaerobic growth. Since the *cidABC* operon had previously been shown to affect metabolite transport, *cidA*, *cidB* and *cidC* mutants were also tested under these same conditions. As shown in Figure 3-7, no differences in growth were observed, indicating that this operon does not affect the utilization of pyruvate.

Based on the results generated by this study and others [29, 56, 57], one could speculate that these two operons work in concert, one to transport pyruvate into the cell for the substrate of the *cid* operon. However, testing of extracellular acetate and acetoin levels during carbon overflow conditions (35 mM) revealed that the *lrg* mutation does not affect the product of these metabolites (data not shown). One caveat of these experiments is that the amount of acetate generated during overflow metabolism conditions by the Pta-AckA pathway overshadows the effects of the *cidABC* or *lrgAB* mutations acetate production. Thus, we generated the *cidABC* mutations in a *pta*/*ackA* mutant background and were able to demonstrate the effects of the *cidABC* mutations on acetate production [56]. However, we have been unable to generate either *lrgA/ackA* or *lrgA/pta* mutants to date. One possible

reason for this is that the *pta* and *ackA* mutations result in elevated levels of pyruvate in the cytoplasm [13] and the *lrgAB* operon is important for regulating the amount of pyruvate within the cell. In eukaryotic cells, the amount of pyruvate within the mitochondria is known to be tightly regulated, as too much or too little of this important metabolite leads to a disease state [21]. In fact, medicines that block the import of pyruvate into the mitochondria are being used to treat these illnesses including Parkinson disease and diabetes [4]. In this respect, there are conflicting reports on whether the *lrgAB* homologs have the ability to act as a pyruvate exporter as well. In *Bacillus subtilis*, pyruvate can be exported via the *lrgAB* homologs, but they do not appear to play this role in *Streptococcus mutans* [59, 61]. The ability of the *S. aureus lrgAB* operon to export pyruvate remains to be determined and is the subject of our current investigations.

Chapter 4 The *lrgAB* operon is important for pyruvate utilization

Introduction

Pyruvate is a key central molecule of basic metabolism. It is the end product of glycolysis and its final fate is dependent on the conditions with which the organism is growing. If the pyruvate generated from one glucose enters the TCA cycle, it has the ability to generate roughly 38 molecules of ATP [4]. However, in the absence of oxygen, where the TCA cycle is inactive, pyruvate can be utilized to maintain the redox state of the cell or even converted back to sugars needed for DNA and RNA replication through gluconeogenesis.

Staphylococcus aureus has the ability to adapt to and cause infection in many different niches within the body [78]. One of the reasons it is such a successful pathogen is its vast array of virulence factors that it utilizes to manipulate the environment to provide the necessary nutrients for survival. Another reason for its success is its ability to alter its metabolic state and grow or survive within these different niches [10]. *S. aureus* encodes numerous transcriptional regulators that sense the environment (e.g. nutrients, stressors, etc.) and then alter its metabolome. For example, the well-studied carbon catabolite response regulator, CcpA, is important for regulating carbon flow through glycolysis when preferred carbon sources are available [10]. While other regulators like CodY, Rex, and SrrAB alter gene expression by sensing branch chain amino acids and GTP, the redox status of the cell and the oxygen availability, respectively [7, 10].

LytSR is a two-component regulatory system, where LytS is the membrane bound sensor kinase that when activated phosphorylates its cognate response regulator, LytR, that then alters downstream gene expression through binding to promoter regions of its target genes [65]. Like many other two-component systems, LytS can fine tune the activity of the response regulator [65] dependending on the state of the cell. Microarray studies revealed that LytSR differentially regulates around 267 genes that are involved in carbohydrate, energy and nucleotide metabolism [79], with expression of *lrgAB*, the likely primary target, being LytSR dependent [64]. Additionally, Lehman et al, elegantly demonstrated that Asp53 is the necessary phosphorylation site of LytR that then binds to the promoter region of *lrgAB* [65].

While the conditions that are able to induce *lrgAB* expression through LytSR have been identified, the actual signal that LytS senses remains to be elucidated. Previous experiments have shown that agents that dissipate membrane potential (i.e. CCCP and gramicidin) as well as weak acids induce *lrgAB* expression in a *lytSR*-dependent manner [65, 66, 69]. *S. aureus* has the ability to grow under microaerobic and anaerobic conditions where membrane potential is decreased [80]. The *lrgAB* operon is also highly induced in a *lytSR*-dependent manner during microaerobic conditions (Figure 3-10), suggesting that low oxygen environments might be where the *lrgAB* operon may have a significant impact on *S. aureus*.

Similar to the *B. subtilis* and *S. mutans* homologues, the *S. aureus lrgAB* operon, as demonstrated in Chapter 3, has been reported to be a transporter of pyruvate during micro- and/or anaerobic conditions. In fact, the *lrgAB* mutant is unable to grow at all under anaerobic conditions and those amino acids that generate pyruvate, serine, threonine,

glycine and alanine, are not consumed, suggesting that the pyruvate is a necessary source of ATP generation under these conditions. Additionally, experiments of a *lrgAB* promoter fusion suggest that LytS is possibly sensing changes in Qox, the terminal cytochrome and that CcpA is an inducer of *lrgAB* via regulation of *lytSR*. Finally, despite no noticeable growth phenotype, metabolite analysis of aerobic cultures reveals that the *lrgAB* operon may also alter the metabolic processes of the cell under these conditions.

Results

A lrgAB mutant is less sensitive to 3-fluoropyruvic acid

In *E. coli* the synthetic pyruvate analog 3-bromopyruvate and 3-fluoropyruvate competitively inhibit pyruvate uptake in whole cells as well as membrane vesicles [81]. Uptake by natural analogs, such as alanine and lactate showed very low affinity for blocking this uptake suggesting that this inhibition is due to the similar structure of the synthetic analogs to pyruvate [81]. Additionally, research in eukaryotic systems utilize 3-fluoropyruvate to inhibit the pyruvate dehydrogenase complex by competitively binding to the active site of the enzyme [82]. The *S. aureus lrgAB* operon has been implicated in pyruvate transport and in a complementary test of the ability of the *lrgAB* mutant to import pyruvate, we grew the wild type, *lrgAB* mutant, and complemented strain in CDM with pyruvate as the sole carbon source under microaerobic conditions in the presence of increasing concentrations of 3-fluoropyruvic acid. As can be seen in Figure 4-1 the *lrgAB* mutant has a significantly decreased sensitivity to this toxic pyruvate analog. The decreased sensitivity to this compound suggests that the *lrgAB* operon is involved in 3-fluoropyruvic acid import.

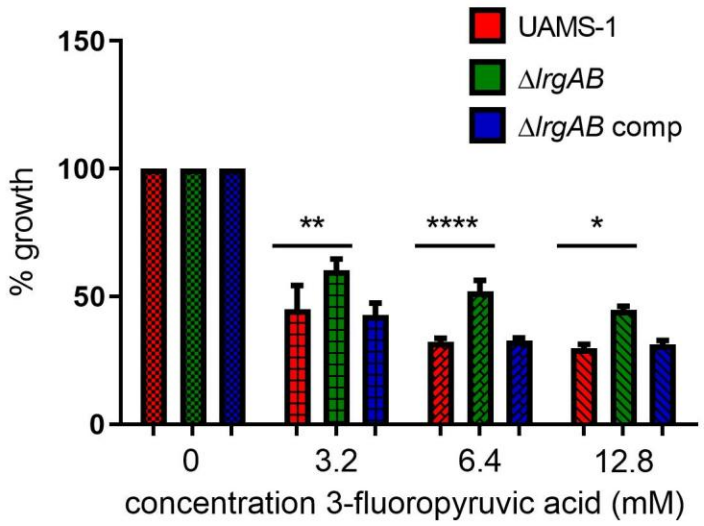

Figure 4-1 Effect of the *lrgAB* mutation on 3-fluoropyruvic acid toxicity.
S. aureus UAMS-1, the *lrgAB* mutant, and the complemented strain were grown under microaerobic conditions in CDM containing 30 mM pyruvate and increasing concentrations of 3-fluoropyruvic acid.

The inability of the lrgAB mutant to grow during anaerobic conditions is not due to lowered respiration

While the *lrgAB* mutant exhibits diminished growth under microaerobic conditions, it cannot grow at all when cultured in anaerobic conditions (Figure 4-2). Due to the lack of a phenotype of this mutant during aerobic growth in CDM with pyruvate as the sole carbon source, we speculated that a respiration-dependent pyruvate transporter might be active during aerobic growth. To test the role respiration has on the pyruvate import, 3 mM nitrate was added as a terminal electron acceptor to cultures that were grown in the anaerobic chamber with pyruvate as the sole carbon source and growth was assessed after 24 hours. The addition of nitrate to the cultures increased growth of both the wild type and mutant but it did not restore the growth of the *lrgAB* mutant to wild type levels (Figure 4-3). These data suggest that the pyruvate transport during aerobic conditions is not due to just active respiration, the possibility that this other transporter is not expressed under anaerobic conditions should been assessed.

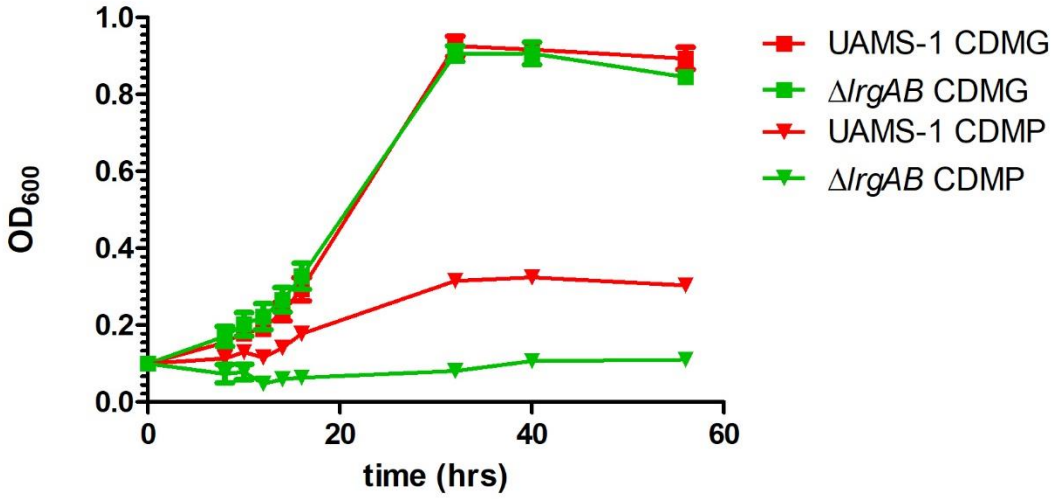

Figure 4-2 Effect of the *lrgAB* operon on growth on pyruvate under anaerobic conditions. UAMS-1 and the *lrgAB* mutant were inoculated into conditioned, chemically defined, media (CDM) containing either 30 mM pyruvate (P) or 14 mM glucose (G) in a Coy anaerobic chamber. Growth was monitored (OD_{600}) for 56 hrs.

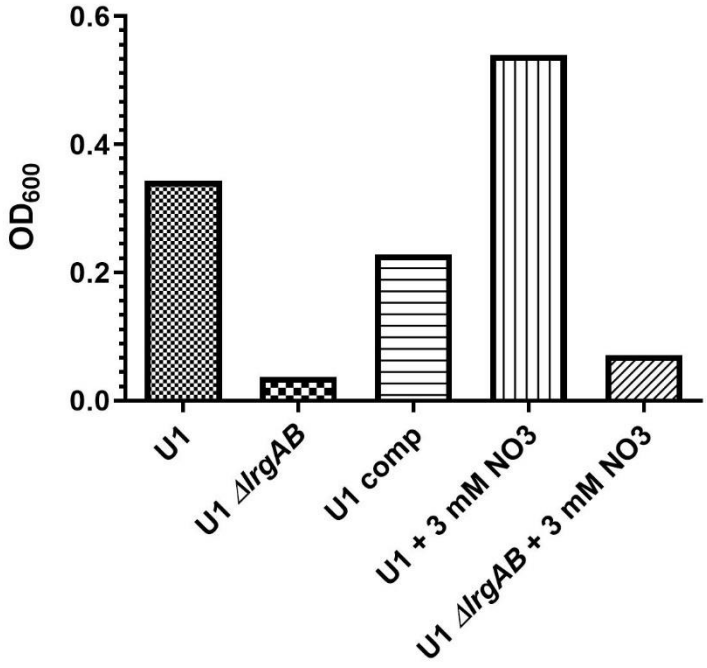

Figure 4-3 Respiration increases growth of wild type but not rescue the *lrgAB* mutant UAMS-1, *ΔlrgAB* and *ΔlrgAB* complement strains were grown in an anaerobic chamber in CDM + 30 mM pyruvate with and without 3 mM nitrate. Optical density was used as a measure of growth after 24 hours.

Amino acids that generate pyruvate are not consumed during anaerobic growth

S. aureus cultured in CDM media lacking any carbon source utilizes alanine, glycine, threonine and serine through the pyruvate node to generate acetate and ATP via the Pta-AckA pathway [83]. Halsey *et al*. reported that anaerobic growth of wild-type bacteria in CDM media with only amino acids was dependent on the addition of lactate or nitrate to act as a terminal electron acceptor. Since the *lrgAB* mutant was unable to grow under anaerobic conditions when pyruvate was the sole carbon source it was speculated that those amino acids that generate pyruvate were not consumed under these conditions. To assess the role that amino acids have during anaerobic growth, amino acid analysis was performed on exponential and stationary phase cultures of the wild-type strain grown in CDM under aerobic and anaerobic conditions with either glucose or pyruvate as the sole carbon source. In agreement with previous reports, those amino acids that generate pyruvate (e.g. alanine, glycine, threonine, and serine) are not consumed under anaerobic conditions with pyruvate as the primary carbon source (Figure 4-4) similar to amino acid consumption from media with no carbon source. The inability for wild-type bacteria to consume amino acids for anaerobic growth with pyruvate as the sole carbon source is in agreement with the lack of growth of the *lrgAB* mutant under these same conditions, where wild-type cells are able to use pyruvate for energy production the *lrgAB* mutant cannot consume the pyruvate or amino acids.

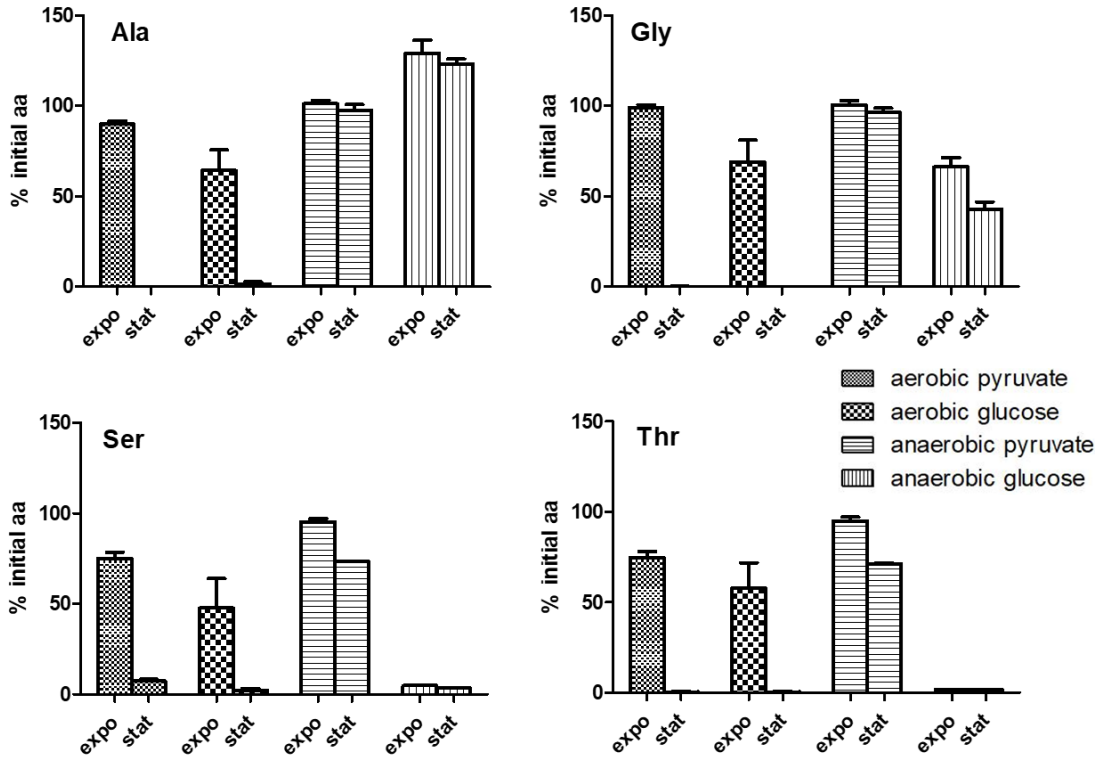

Figure 4-4 Pyruvate generating amino acids are not utilized during anaerobic growth on pyruvate.
S. aureus UAMS-1 cells were grown under aerobic or anaerobic conditions in either CDM + 14 mM glucose or CDM + 30 mM pyruvate. Samples were collected at either exponential or stationary phase of growth. Percent of initial amino acids added to cultures for alanine, glycine, serine or threonine.

CcpA is a positive regulator of lrgAB through LytSR

As a key central metabolite, the steady state control of pyruvate pools is important for growth and survival. The carbon catabolite repressor, CcpA, regulates gene expression by binding to specific sequences within the genes promoter region (*cre* sites) in response to the availability of primary carbon sources [84]. Pyruvate enters the metabolic pathway after the steps which alter CcpA activity, therefore it was assumed that pyruvate uptake would not occur until the preferred carbon sources were consumed and that this would occur through CcpA activity on the *lrgAB* operon. Additionally, a *cre* site and CcpA binding was shown to occur in the promoter region of *lrgAB* homologues in *Bacillus subtilis* and *Streptococcus mutans* [59, 85]. Interestingly, analysis of the *S. aureus lrgAB* promoter region revealed a lack of a consensus *cre* site (Figure 4-5). However, analysis of the *lytSR* promoter region revealed a possible *cre* box with only one mismatch to the consensus sequence (Figure 4-5) upstream of the *lytS* and another before the *lytR* start site leading to the hypothesis that CcpA mediates the carbon source regulation of *lrgAB* expression through the *lytSR* two-component system. To test this hypothesis, a plasmid with the *lrgAB* promoter region cloned upstream of a GFP (pEM80) was introduced into a *ccpA* mutant as well as the wild-type strain [33]. These isolates were analyzed for growth and GFP expression in media with either glucose, pyruvate or glucose and pyruvate. As can be seen in Figure 4-6, there is less GFP in the *ccpA* mutant compared to the wild type in all conditions tested revealing that CcpA is acting as an activator of the *lrgAB* operon.

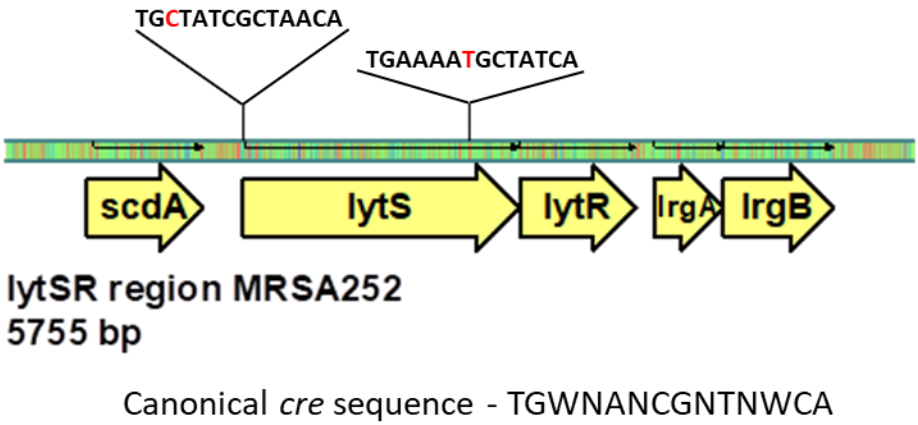

Figure 4-5 Identification of cre site within *lytSR* and *lrgAB* operons.
The MRSA252 *lytSR* and *lrgAB* region of the genome was assessed for possible *cre* sites using the canonical sequence TGWNANCGNTNWCA. Two *cre* sites with one mismatch each were identified and are labelled in the diagram.

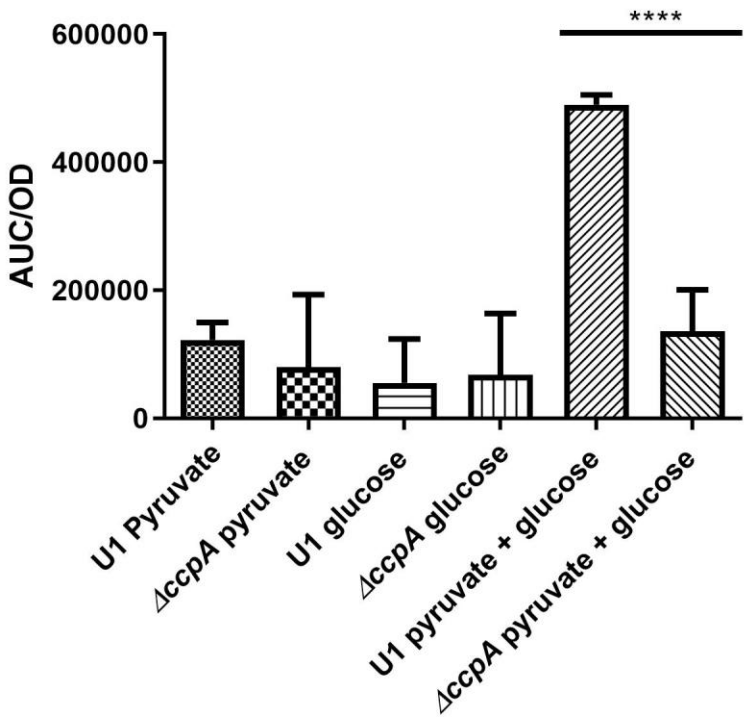

Figure 4-6 CcpA is a positive regulator of *lrgAB* expression
UAMS-1 or the *ccpA* mutant carrying pEM80 were grown in a 96-well microtiter plate on a Tecan plate reader where OD_{600} and GFP units were measured every 30 minutes for 24 hours. Area under the curve analysis was completed for both and graphed as AUC fluorescence per AUC OD for growth in CDM + 7.5 mM glucose + 15 mM pyruvate, CDM + 30 mM pyruvate or CDM + 15 mM glucose.

The Qox terminal cytochrome activity affects lrgAB expression

A cells proton motive force (PMF) is a product of two components: the pH gradient across the cell membrane (ΔpH) and the membrane potential (Δψ) [86, 87]. It has been shown that *lrgAB* expression is induced through the LytSR two-component regulatory system when the membrane potential is dissipated by carbonyl cyanide m-chlorophenylhydrazone (CCCP) [65, 66]. However, the exact element that LytS is actually sensing is unknown. To assess the possible role of different components of the electron transport chain might have on *lrgAB* expression, mutants from the Nebraska Transposon Mutant Library (NTML) were transformed with pEM80 and examined. Due to the fact that the NTML is generated in the JE2 background, a transposon mutant inserted into *lrgA* was assessed for growth in CDM with pyruvate as the sole carbon source and the same phenotype observed in the UAMS-1 background was detected (Figure 4-7). Transposon mutations within the genes encoding NADH dehydrogenase I or II (SAUSA300_0841 or SAUSA300_0844), succinate dehydrogenase (*sdhA*), terminal oxidases *qox* and *cydA*, as well as the ATPase alpha subunit, *atpA* were analyzed by measuring the amount of GFP produced over the entire growth period and compared to that produced by the JE2 (pEM80) strain. When grown in media with glucose as the sole carbon source, none of the mutants tested showed a difference in GFP expression compared to JE2 (Figure 4-8B). However, there was a 3-fold increase in the GFP detected in the *qox* terminal oxidase (Figure 4-8A) when grown in media with pyruvate as the sole carbon source. Consistent with CCCP dissipation, these data suggest that LytS might be sensing the state of the Qox terminal oxidase and not alterations in ATP levels.

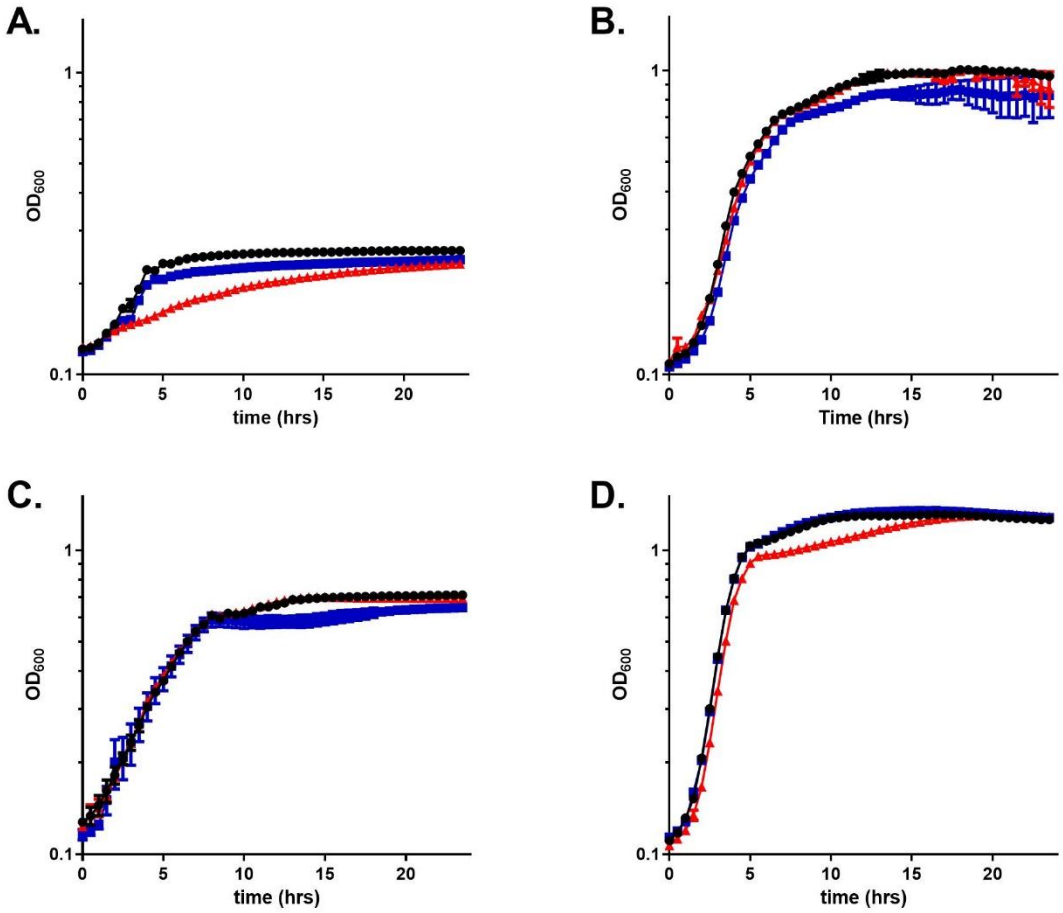

Figure 4-7 *S. aureus* JE2 *lrgA* transposon mutant has same growth defect during microaerobic growth with pyruvate as the sole carbon source.
Growth curves of *S. aureus* JE2 (black circles), JE2 *lrgA*::ΦNE (red triangles), and JE2 *lrgA*::ΦNE with pJE31 (blue diamonds) in (A) CDM with 30 mM pyruvate covered with oil, (B) CDM with 30 mM pyruvate, (C) CDM with 15 mM glucose covered with oil, and (D) CDM with 15 mM glucose.

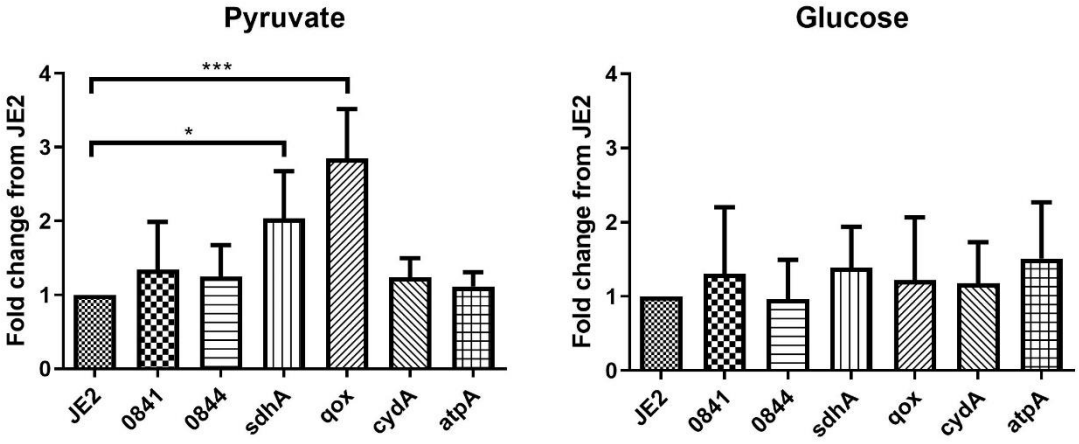

Figure 4-8 Electron transport chain mutations affect *lrgAB* expression.
Transposon mutants of the electron transport chain carrying a *lrgAB* transcriptional reporter (pEM80) were grown in CDM with (A) pyruvate or (B) glucose as the sole carbon source. GFP production was measured every 30 minutes and area under the curve analysis was performed and compared to the wild type.

The lrgAB operon affects the metabolite profile during aerobic growth.

During aerobic growth when glucose is used as the carbon source it is converted to pyruvate through glycolysis. While these conditions are used to assess fitness of mutants it may not be the conditions to which *S. aureus* is exposed in a host. In fact, the amount of glucose present in the nares is significantly lower than the 4-8 mM present in human blood while the amount of pyruvate is significantly higher [88]. The *lrgAB* mutant does not have a growth defect when grown under aerobic conditions (Figure 4-10), suggesting that there is another transporter of pyruvate under these conditions. Also, the fact that CcpA appears to be an activator of *lrgAB* suggests that pyruvate would be consumed in media with both glucose and pyruvate present. To test this possibility, the wild type, *lrgAB* mutant and complement isolates were grown under aerobic conditions in either glucose alone, pyruvate alone, or glucose and pyruvate as the carbon source. As shown in Figure 4-10 and Figure 4-11, there were no differences seen in the growth kinetics, pyruvate consumption, glucose consumption or acetate generation when these strains were grown in either glucose alone or pyruvate alone. Even though no growth defect was observed for the *lrgAB* mutant grown with glucose and pyruvate, there was roughly 5 mM less acetate generated which coincided with pyruvate remaining in the media (Figure 4-9). Interestingly, this difference in acetate generation, resulted in the cell's ability to consume the acetate during stationary phase. These data suggest that *lrgAB* has a role in pyruvate consumption during aerobic growth conditions and is in agreement with CcpA being an activator of *lrgAB* expression due to the consumption of pyruvate at the same time as glucose.

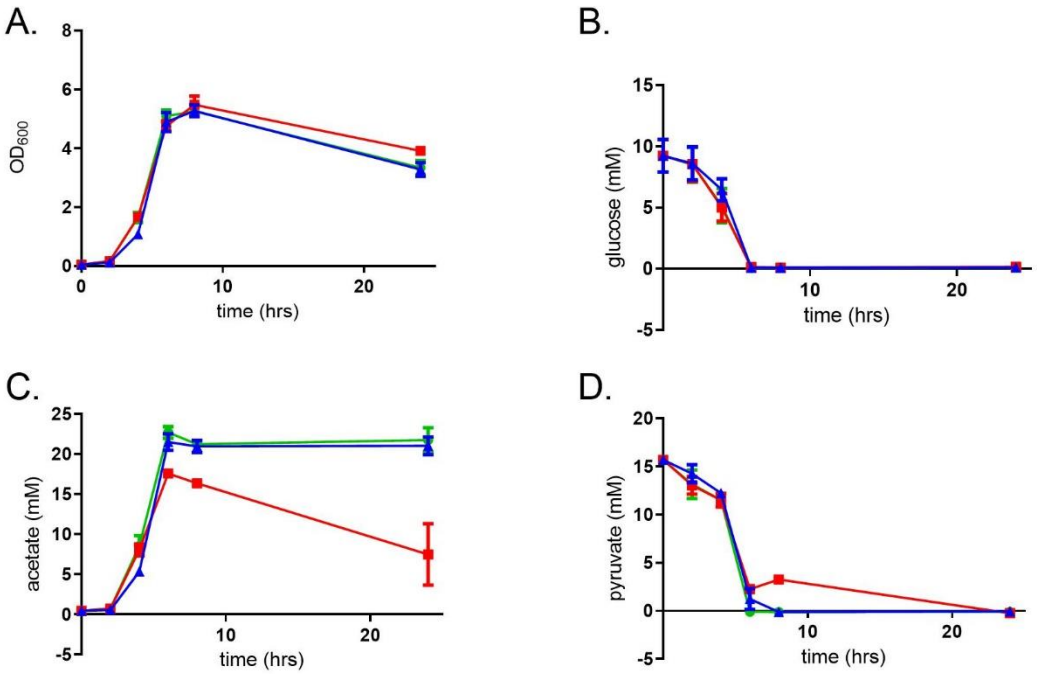

Figure 4-9 The *lrgAB* operon affects metabolic byproducts during growth with glucose and pyruvate

Aerobic grown UAMS-1 (green circles), UAMS-1 *ΔlrgAB* (red squares) and UAMS-1 *ΔlrgAB* with pJE30 (blue triangles) in CDM with 15 mM pyruvate and 7.5 mM glucose were sampled every 2 hours for (A) growth, (B) extracellular glucose, (C) acetate and (D) pyruvate.

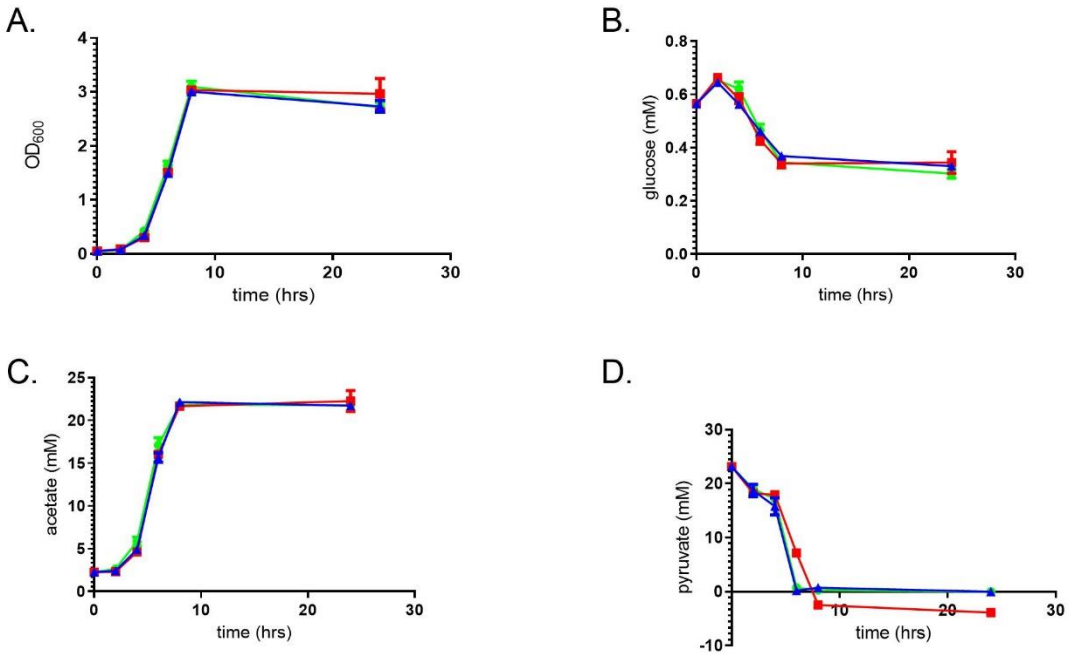

Figure 4-10 Growth and metabolite analysis with pyruvate as the sole carbon source Aerobic grown UAMS-1 (green circles), UAMS-1 *ΔlrgAB* (red squares) and UAMS-1 *ΔlrgAB* with pJE30 (blue triangles) in CDM with 30 mM pyruvate were sampled every 2 hours for (A) growth, (B) extracellular glucose, (C) acetate and (D) pyruvate.

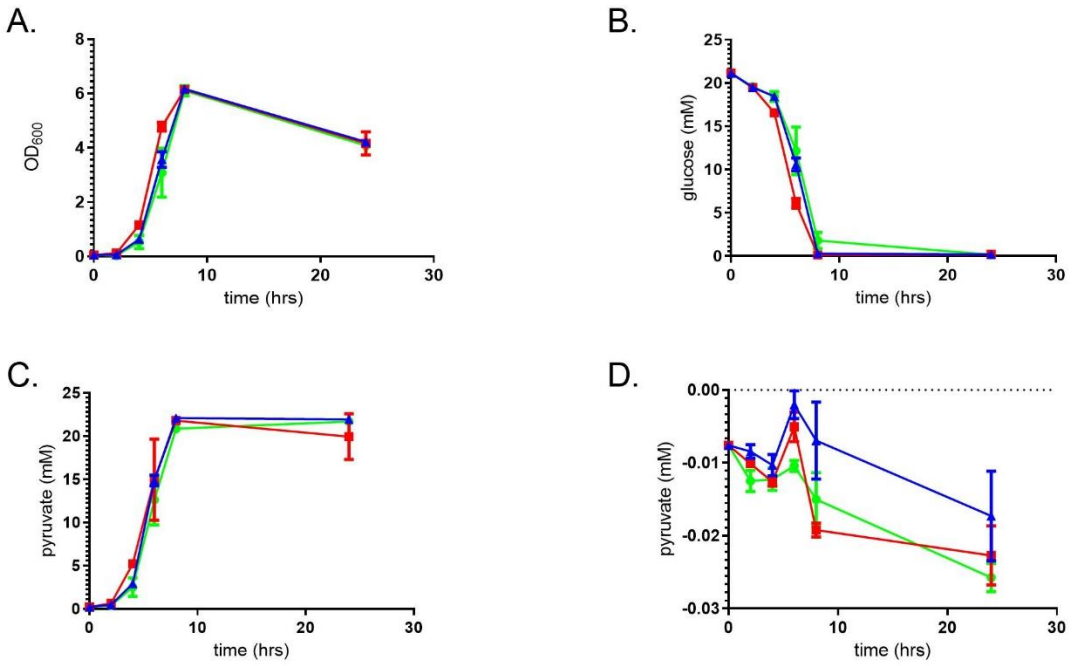

Figure 4-11 Growth and metabolites analysis in CDM with glucose as the sole carbon source

Aerobic grown UAMS-1 (green circles), UAMS-1 *ΔlrgAB* (red squares) and UAMS-1 *ΔlrgAB* with pJE30 (blue triangles) in CDM with 15 mM glucose were sampled every 2 hours for (A) growth, (B) extracellular glucose, (C) acetate and (D) pyruvate.

Discussion

The ability of *S. aureus* to adapt to different niches within hosts is not only due to the vast array of virulence factors it produces [89], but also due to its ability to alter its metabolic state by sensing the environment with which it occupies [5, 10, 90]. Bacteria rely heavily on two-component regulatory systems to alter their virulence factor production in response to cues from their environment [91]. Recently, it has been revealed that *S. aureus* responds to pyruvate by altering virulence factor expression [92]. Pyruvate is an essential molecule in metabolism and as the end product of glycolysis it has the ability to be fermented to lactate, acetate, 2,3-butaindiol, and ethanol or it can enter the TCA cycle where it is completely decarboxylated and feeds the electron transport chain during respiration [3]. In addition, *S. aureus* grown in conditions with limited preferred carbon sources have a decreased respiration rate that results in a necessity for the TCA cycle intermediate, 2-oxoglutarate, as well as ATP generation through the Pta/AckA pathway [83].

Consistent with the need for a preferred carbon source or consumption of amino acids, which requires a large amount of ATP, the *S. aureus lrgAB* mutant is unable to grow under anaerobic conditions with pyruvate as the sole carbon source (Figure 4-2). Due to the *lrgAB* mutant not having a growth defect when grown under aerobic conditions we speculated that with a higher respiration rate the mutant was able to utilize those amino acids that generate pyruvate, serine, threonine, alanine and glycine, which are not consumed under anaerobic growth (Figure 4-4). However, the addition of nitrate as an electron acceptor anaerobically increased growth of the wild-type strain did not

significantly alter growth of the *lrgAB* mutant (Figure 4-3) suggesting that there is another pyruvate transporter produced during aerobic growth.

The *S. aureus* genome encodes 16 two-component regulatory systems that sense and respond to the environment [93]. The LytSR two-component regulatory system induces the *lrgAB* operon in response to dissipation of membrane potential [65, 66]. Lehman et al., revealed that the *lrgAB* induction to membrane dissipation is dependent on LytS-mediated signaling [65]. Analysis of transposon mutants of the electron transport chain carrying the promoter fusion for the *lrgAB* operon (pEM80), revealed that, Qox, the terminal electron acceptor may be what LytS is sensing during growth with pyruvate as the sole carbon source (Figure 4-8).

Finally, the major regulator of the carbon catabolite response, CcpA, has been shown to regulate gene expression in response to preferred carbon sources [94]. Since pyruvate is not a PTS sugar we speculated that CcpA may be a repressor of *lrgAB* expression by binding to *cre* sites within the *lrgAB* promoter as has been shown in *B. subtilis* [59] and *S. mutans* [85]. Interestingly, *lrgAB* promoter activity was reduced in a *ccpA* mutant which suggests that CcpA is an activator of the *lrgAB* operon through *lytSR* (Figure 4-6). In agreement with CcpA being an activator of *lrgAB* expression, glucose and pyruvate were simultaneously removed from the media of a wild-type culture when grown under aerobic conditions. Analysis of the *lrgAB* promoter region did not identify a *cre* site within the *lrgAB* promoter region. However, analysis of the *lytSR* sequence revealed a *cre* site just upstream of the start site of *lytS* as well as a second upstream of *lytR* suggesting that CcpA regulation of *lrgAB* expression may be mediated via regulation of *lytSR*.

S. aureus has the ability to adapt to and cause disease in many different niches within the body [78, 95]. The ability for bacteria to utilize all sources of energy within different niches would clearly be beneficial to their long-term survival. These data support recent reports that the *lrgAB* operon is important for the transport of pyruvate and shed light on the possible conditions that induce *lrgAB* expression and what specific aspect of respiration LytS is likely to sense. As more information on environmental conditions within different infections becomes available the importance of pyruvate signaling and utilization will come to light.

Chapter 5 Concluding remarks

Future directions

Identify the genes supporting growth on pyruvate during aerobic growth

The lack of a growth defect in the *lrgAB* mutant during aerobic growth with pyruvate as the sole carbon source suggests the presence of another protein that has the ability to import pyruvate. It is possible that this other protein is a non-specific transporter that is expressed under these specific conditions but not during low oxygen growth conditions. Selecting for mutants that have the ability to grow in the presence of the toxic analog, 3-fluoropyruvic acid could be one way to identify this secondary transporter. The genomes of these isolates could then be sequenced to identify genes potentially responsible for the aerobic pyruvate consumption. If spontaneous mutants cannot be obtained, a second way to identify this aerobic transporter would be to screen the NTML for the loss of aerobic growth in CDM with pyruvate as the primary carbon source.

Labelled pyruvate uptake studies

While the experiments performed in chapters 3 and 4 suggest that the *lrgAB* operon is necessary for import of pyruvate during low oxygen conditions, direct evidence showing this is still needed. One limitation of these experiments is that pyruvate utilization is being assessed using cells that are not growing as well as the wild-type strain (Figure 3-9). To overcome this limitation, we performed the experiments supplementing the growth media with glucose (data not shown), however, interpretation of these data is difficult because the addition of glucose more than likely results in large alterations of metabolic gene expression due to activity of the major regulators of carbon catabolite repression. To confirm that the *lrgAB* operon is in fact a pyruvate transporter, experiments need to be

performed where cells are grown under microaerobic conditions and then ^{14}C labelled pyruvate is introduced to assess the ability of these strains to internalize the labelled pyruvate. As a control, we would also use the 3-fluoropyruvic acid to compete for uptake in the wild-type cultures, similarly to what has been done for *E. coli* [81].

Additionally, results using *B. subtilis* suggest that the *lrgAB* operon can also affect the export of pyruvate when internal levels are too high [59]. To assess pyruvate export, the *lrgAB* mutation can be combined with a *cidC* or *pta/ackA* mutations, which cause high intracellular and extracellular levels of pyruvate [13, 76]. Once these double mutants are generated the amount of extracellular pyruvate could be measured to assess the possible role *lrgAB* has on the export of pyruvate.

Biofilm studies

Bacterial biofilm creates an environment where many different niches arise. The *S. aureus cid* and *lrg* operons role during this development has been extensively studied [33, 65, 68, 96] and fluorescence reporters have revealed that *cid* and *lrg* expression is located within distinct tower structures [33]. Additionally, differences in *lrgAB* expression in biofilms generated by a *lytSR* mutant revealed that the expression within the towers is LytS-dependent [65]. Also, overexpression of *lytS* or *lytR* resulted in constitutive *lrgAB* expression in the biofilm that by Comstat analysis showed thicker, and smoother biofilm production [65]. While initial experiments analyzing a *lrgAB* mutant biofilm grown under flow conditions did not reveal any dramatic phenotype, it would be interesting to test whether the biofilm phenotype produced by the *lytS* or *lytR* mutants was dependent on *lrgAB*. Finally, it would be interesting to determine the importance of the *lrgAB* expression

within the towers. Could this be a signaling pathway that *S. aureus* is using to affect the niche specific gene expression in neighboring cells?

Animal work

While the biological relevance of a pyruvate transporter is clear in eukaryotes, where disease arises when pyruvate levels between the cytosol and mitochondria are imbalanced, the need for such control in prokaryotes is not as clear since metabolism is not compartmentalized. However, the research presented above suggests that there are conditions that require a pyruvate specific transporter. While more information is starting to be available on nutrient availability between different host niches, much remains to be learned about the specific nutritional requirements during infections. One model of infection where pyruvate fermentation to lactate has been shown to be important is the prosthetic joint infection model (PJI). Heim et al. revealed that *S. aureus* generated lactate results in IL-10 production leading to an altered immune response and chronic infections [97]. This is also an infection that would not have much glucose from the blood suggesting it may be a condition where pyruvate transport could be important. Preliminary experiments support this idea as the *lrgAB* mutant has decreased survival after seven days (Figure 5-1). Repeat experiments following the infection for a longer period of time as well as completing flow cytometry data of the immune response remain to be completed.

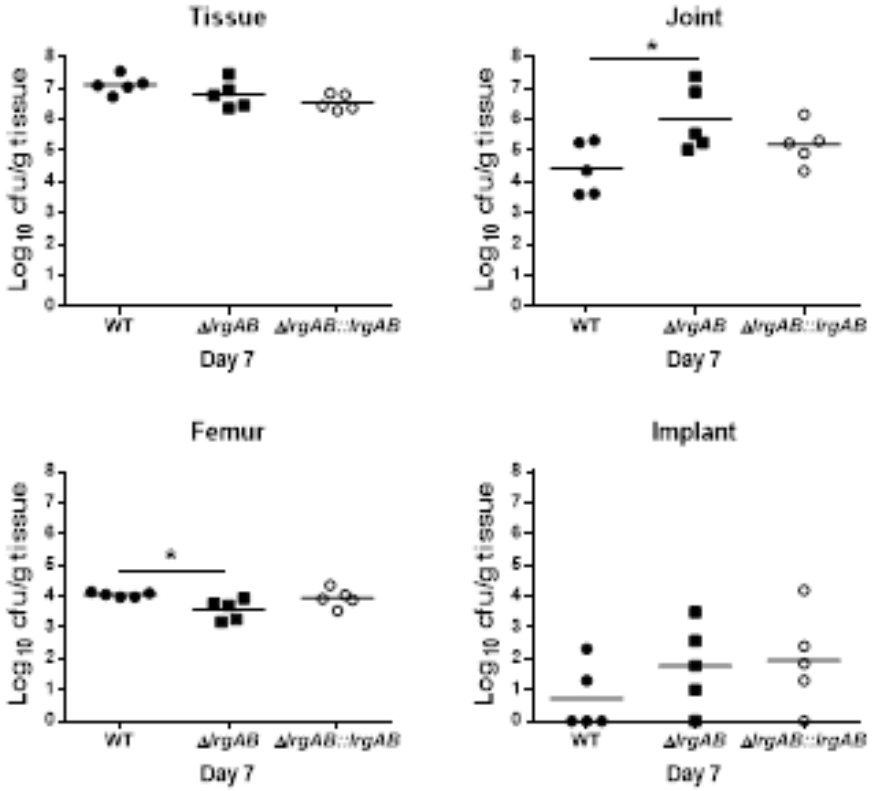

Figure 5-1 The *lrgAB* mutant in the prosthetic joint infection model
Roughly 1x10^3 colony forming units of UAMS-1, *lrgAB* mutant and complement isolates were inoculated onto the end of the pin in the PJI model. After 7 days the tissue, joint, femur and implant were collected and plated for colony forming units.

Chapter 6 Conclusions

While the enzymatic processes that produce or utilize pyruvate to generate energy (ATP) are similar between the different kingdoms of life, there are a few major differences. One of the biggest is that metabolism in eukaryotic cells is compartmentalized, while in bacteria all these processes occur in the cytosol. Pyruvate is an important intermediate to the metabolic processes within the cell and its fate is determined by the environment the cell encounters. It can generate energy by entering the TCA cycle through acetyl-CoA and continuing through aerobic respiration, it can be fermented by mixed acid fermentation when oxygen levels are low. It can provide essential amino acids and it can even be converted back to carbohydrates through gluconeogenesis. Pyruvate metabolism provides the essential molecules needed for a living cell and the complexity of the regulation of the pyruvate levels within the cell should be appreciated as many eukaryotic diseases are associated with the dysregulation of the pyruvate node of metabolism and the MPC1/MPC2 carriers. Recently, homologs of the *lrgAB* operon of *S. aureus* have been shown to be important for pyruvate utilization under certain growth conditions. Interestingly, these proteins share many common features with the eukaryotic mitochondrial pyruvate carriers and is a source for future experimentation.

While, the flow of carbon through the pyruvate node in both eukaryotes and prokaryotes is similar, one of the most notable differences is the compartmentalization that occurs in the eukaryotic cell. Due to this compartmentalization, the necessity for the cell to encode a specialized protein for pyruvate transport is necessary, while in prokaryotes the processes that generate and utilize pyruvate occur within the cytosol. The ability for the cell to utilize all sources of energy from its environment, including pyruvate, may allow

for prokaryotic cells, including *S. aureus*, to survive in niches that it would otherwise be unable to without the means to internalize this key nutrient.

Recent research on the *Bacillus subtilis pftAB* and *Streptococcus mutans lrgAB* operons revealed that they are necessary for the import of pyruvate [59-61]. These homologues of the *S. aureus lrgAB* operon exhibit a decrease in pyruvate utilization under specific conditions and phases of growth. The *lrgAB* genes encode membrane proteins that have previously been shown to be involved in the control of murein hydrolase activity and programmed cell death (PCD) [52]. The LrgA and LrgB proteins of *S. aureus* are 15.7- and 25- kDa in size, respectively. They are predicted hydrophobic membrane proteins, LrgA is predicted to have three to four transmembrane domains while LrgB is predicted to have seven.

The LrgAB proteins from *S. aureus*, *B. subtilis* and *S. mutans* all share many structural features with the mitochondrial pyruvate carriers, MPC1 and MPC2. They have similar sizes; they are hydrophobic membrane proteins and oligomerize with each other to form higher molecular weight complexes. Also, like the MPC1/MPC2 proteins, the *B. subtilis lrgAB* homologs are both necessary for the import of pyruvate [60], similar to that of *S. aureus lrgAB*. Finally, the *lrgAB* operon is induced through the LytSR two-component regulatory system in response to dissipation in membrane potential. Interestingly the MPC1 and MPC2 proteins ability to transport pyruvate are altered by changes in oxygen consumption and compounds that increase membrane potential, such as FCCP [26].

While plant metabolism was not discussed in detail, photorespiratory carbon flux is necessary for recycling glycolate-2-phosphate for the regeneration of RubisCO. Photorespiration is a compartmentalized process that occurs between the cytosol,

chloroplasts, peroxisomes and mitochondria and there are six transport steps that are necessary for this process to occur [58]. Interestingly, the plant homolog of *S. aureus lrgAB*, PLGG1, in *Arabidopsis thaliana* has been identified as the transporter necessary for transporting the two and three carbon molecules, glycolate and glycerate, across the chloroplast envelope during photorespiration [58]. These results indicate that proteins encoded by the *lrgAB* operon and its homologues are broadly conserved transporters of small sugars.

Finally, the proapoptotic Bcl-2 family of proteins that are necessary for the caspase cascade resulting in apoptosis of the mitochondria, Bax and Bak also share similar characteristics, including their ability to function like holins [45]. While this family of Bcl-2 proteins have been shown to be necessary for the apoptotic process, there have been numerous reports that they have other cellular functions. These functions include regulating mitochondrial shape, regulating mitochondrial permeability and inner mitochondrial membrane metabolism, controlling calcium homeostasis, regulation of the unfolded protein response, regulation of glucose and lipid metabolism, regulation of macroautophagy and mitophagy, and regulation of DNA damage response [98]. While not all Bcl-2 family of proteins play a role in all of these other cellular processes it does show that these classically described cell death proteins are important for other functions within the cell. Atan Gross et al., nicely described these "BCL-2 family members as 'sleeper agents' ready to inform on the state of the cell in their clandestine, night job as an agent of cell death" [98], which makes one wonder if this similarly describes the *cidABC* and *lrgAB* operons of *S. aureus* as possibly having different "night jobs" that either lead to survival or target them for PCD.

Chapter 7 Bibliography

1. *Organic chemistry.* Journal of the Chemical Society, Abstracts, 1878. **34**(0): p. 19-82.
2. Kluyver, A.J. and H.J.L. Donker, *Die Einheit in der Biochemie*. 1926: Borntraeger.
3. Jurtshuk, P., Jr., *Bacterial Metabolism*, in *Medical Microbiology*, S. Baron, Editor. 1996, University of Texas Medical Branch at Galveston

Copyright © 1996, The University of Texas Medical Branch at Galveston.: Galveston (TX).

4. Zangari, J., et al., *The Multifaceted Pyruvate Metabolism: Role of the Mitochondrial Pyruvate Carrier.* Biomolecules, 2020. **10**(7).
5. Balasubramanian, D., et al., *Staphylococcus aureus pathogenesis in diverse host environments.* Pathog Dis, 2017. **75**(1).
6. Seidl, K., et al., *Effect of a glucose impulse on the CcpA regulon in Staphylococcus aureus.* BMC Microbiol, 2009. **9**: p. 95.
7. Majerczyk, C.D., et al., *Direct targets of CodY in Staphylococcus aureus.* J Bacteriol, 2010. **192**(11): p. 2861-77.
8. Wolfe, A.J., *The acetate switch.* Microbiol Mol Biol Rev, 2005. **69**(1): p. 12-50.
9. Fuchs, S., et al., *Anaerobic gene expression in Staphylococcus aureus.* J Bacteriol, 2007. **189**(11): p. 4275-89.
10. Somerville, G.A. and R.A. Proctor, *At the crossroads of bacterial metabolism and virulence factor synthesis in Staphylococci.* Microbiol Mol Biol Rev, 2009. **73**(2): p. 233-48.
11. Deutscher, J., et al., *Loss of protein kinase-catalyzed phosphorylation of HPr, a phosphocarrier protein of the phosphotransferase system, by mutation of the ptsH gene confers catabolite repression resistance to several catabolic genes of Bacillus subtilis.* J Bacteriol, 1994. **176**(11): p. 3336-44.
12. Deutscher, J., et al., *Protein kinase-dependent HPr/CcpA interaction links glycolytic activity to carbon catabolite repression in gram-positive bacteria.* Mol Microbiol, 1995. **15**(6): p. 1049-53.
13. Sadykov, M.R., et al., *Inactivation of the Pta-AckA pathway causes cell death in Staphylococcus aureus.* J Bacteriol, 2013. **195**(13): p. 3035-44.
14. Brinsmade, S.R., et al., *Regulation of CodY Activity through Modulation of Intracellular Branched-Chain Amino Acid Pools.* Journal of Bacteriology, 2010. **192**(24): p. 6357-6368.
15. Schlievert, P.M., et al., *Menaquinone analogs inhibit growth of bacterial pathogens.* Antimicrob Agents Chemother, 2013. **57**(11): p. 5432-7.
16. Throup, J.P., et al., *The srhSR gene pair from Staphylococcus aureus: genomic and proteomic approaches to the identification and characterization of gene function.* Biochemistry, 2001. **40**(34): p. 10392-401.
17. Ulrich, M., et al., *The staphylococcal respiratory response regulator SrrAB induces ica gene transcription and polysaccharide intercellular adhesin expression, protecting Staphylococcus aureus from neutrophil killing under anaerobic growth conditions.* Mol Microbiol, 2007. **65**(5): p. 1276-87.
18. Brekasis, D. and M.S. Paget, *A novel sensor of NADH/NAD+ redox poise in Streptomyces coelicolor A3(2).* Embo j, 2003. **22**(18): p. 4856-65.
19. Schell, J.C. and J. Rutter, *The long and winding road to the mitochondrial pyruvate carrier.* Cancer Metab, 2013. **1**(1): p. 6.
20. McCommis, K.S. and B.N. Finck, *Mitochondrial pyruvate transport: a historical perspective and future research directions.* Biochem J, 2015. **466**(3): p. 443-54.

21. Gray, L.R., S.C. Tompkins, and E.B. Taylor, *Regulation of pyruvate metabolism and human disease.* Cell Mol Life Sci, 2014. **71**(14): p. 2577-604.
22. Papa, S., et al., *The transport of pyruvate in rat liver mitochondria.* FEBS Lett, 1971. **12**(5): p. 285-288.
23. Todisco, S., et al., *Identification of the mitochondrial NAD+ transporter in Saccharomyces cerevisiae.* J Biol Chem, 2006. **281**(3): p. 1524-31.
24. Herzig, S., et al., *Identification and functional expression of the mitochondrial pyruvate carrier.* Science, 2012. **337**(6090): p. 93-6.
25. Bricker, D.K., et al., *A mitochondrial pyruvate carrier required for pyruvate uptake in yeast, Drosophila, and humans.* Science, 2012. **337**(6090): p. 96-100.
26. Compan, V., et al., *Monitoring Mitochondrial Pyruvate Carrier Activity in Real Time Using a BRET-Based Biosensor: Investigation of the Warburg Effect.* Mol Cell, 2015. **59**(3): p. 491-501.
27. Gillaspy, A.F., et al., *Role of the accessory gene regulator (agr) in pathogenesis of staphylococcal osteomyelitis.* Infect Immun, 1995. **63**(9): p. 3373-80.
28. Windham, I.H., et al., *SrrAB Modulates Staphylococcus aureus Cell Death through Regulation of cidABC Transcription.* J Bacteriol, 2016. **198**(7): p. 1114-22.
29. Patton, T.G., et al., *The Staphylococcus aureus cidC gene encodes a pyruvate oxidase that affects acetate metabolism and cell death in stationary phase.* Molecular Microbiology, 2005. **56**(6): p. 1664-1674.
30. Sadykov, M.R., et al., *CidR and CcpA Synergistically Regulate Staphylococcus aureus cidABC Expression.* J Bacteriol, 2019. **201**(23).
31. Fey, P.D., et al., *A genetic resource for rapid and comprehensive phenotype screening of nonessential Staphylococcus aureus genes.* mBio, 2013. **4**(1): p. e00537-12.
32. Lee, C.Y., S.L. Buranen, and Z.H. Ye, *Construction of single-copy integration vectors for Staphylococcus aureus.* Gene, 1991. **103**(1): p. 101-5.
33. Moormeier, D.E., et al., *Use of microfluidic technology to analyze gene expression during Staphylococcus aureus biofilm formation reveals distinct physiological niches.* Appl Environ Microbiol, 2013. **79**(11): p. 3413-24.
34. Hussain, M., J.G. Hastings, and P.J. White, *A chemically defined medium for slime production by coagulase-negative staphylococci.* J Med Microbiol, 1991. **34**(3): p. 143-7.
35. Ranjit, D.K., J.L. Endres, and K.W. Bayles, *Staphylococcus aureus CidA and LrgA proteins exhibit holin-like properties.* J Bacteriol, 2011. **193**(10): p. 2468-76.
36. Rigaud, J.L. and D. Lévy, *Reconstitution of membrane proteins into liposomes.* Methods Enzymol, 2003. **372**: p. 65-86.
37. Shafer, W.M. and J.J. Iandolo, *Genetics of staphylococcal enterotoxin B in methicillin-resistant isolates of Staphylococcus aureus.* Infect Immun, 1979. **25**(3): p. 902-11.
38. Lehman, M.K., J.L. Bose, and K.W. Bayles, *Allelic Exchange.* Methods Mol Biol, 2016. **1373**: p. 89-96.
39. Zhu, A., R. Romero, and H.R. Petty, *A sensitive fluorimetric assay for pyruvate.* Anal Biochem, 2010. **396**(1): p. 146-51.
40. Zhu, A., R. Romero, and H.R. Petty, *Amplex UltraRed enhances the sensitivity of fluorimetric pyruvate detection.* Anal Biochem, 2010. **403**(1-2): p. 123-5.
41. Gründling, A., M.D. Manson, and R. Young, *Holins kill without warning.* Proc Natl Acad Sci U S A, 2001. **98**(16): p. 9348-52.
42. Wang, I.N., D.L. Smith, and R. Young, *Holins: the protein clocks of bacteriophage infections.* Annu Rev Microbiol, 2000. **54**: p. 799-825.

43. Raab, R., et al., *Mutational analysis of bacteriophage lambda lysis gene S.* J Bacteriol, 1986. **167**(3): p. 1035-42.
44. Zheng, Y., et al., *Evolutionary dominance of holin lysis systems derives from superior genetic malleability.* Microbiology (Reading), 2008. **154**(Pt 6): p. 1710-1718.
45. Pang, X., et al., *Active Bax and Bak are functional holins.* Genes Dev, 2011. **25**(21): p. 2278-90.
46. Bayles, K.W., *Are the molecular strategies that control apoptosis conserved in bacteria?* Trends in Microbiology, 2003. **11**(7): p. 306-311.
47. Kim, H., et al., *Hierarchical regulation of mitochondrion-dependent apoptosis by BCL-2 subfamilies.* Nat Cell Biol, 2006. **8**(12): p. 1348-58.
48. Antonsson, B., et al., *Bax is present as a high molecular weight oligomer/complex in the mitochondrial membrane of apoptotic cells.* J Biol Chem, 2001. **276**(15): p. 11615-23.
49. Rice, K.C. and K.W. Bayles, *Death's toolbox: examining the molecular components of bacterial programmed cell death.* Mol Microbiol, 2003. **50**(3): p. 729-38.
50. Rice, K.C., et al., *The Staphylococcus aureus cidAB operon: Evaluation of its role in regulation of murein hydrolase activity and penicillin tolerance.* Journal of Bacteriology, 2003. **185**(8): p. 2635-2643.
51. Savva, C.G., et al., *The holin of bacteriophage lambda forms rings with large diameter.* Mol Microbiol, 2008. **69**(4): p. 784-793.
52. Groicher, K.H., et al., *The Staphylococcus aureus lrgAB operon modulates murein hydrolase activity and penicillin tolerance.* J Bacteriol, 2000. **182**(7): p. 1794-801.
53. Rice, K.C., et al., *The Staphylococcus aureus cidAB operon: evaluation of its role in regulation of murein hydrolase activity and penicillin tolerance.* J Bacteriol, 2003. **185**(8): p. 2635-43.
54. Bayles, K.W., *The biological role of death and lysis in biofilm development.* Nature Reviews Microbiology, 2007. **5**(9): p. 721-726.
55. Wang, J. and K.W. Bayles, *Programmed cell death in plants: lessons from bacteria?* Trends Plant Sci, 2013. **18**(3): p. 133-9.
56. Chaudhari, S.S., et al., *The LysR-type transcriptional regulator, CidR, regulates stationary phase cell death in Staphylococcus aureus.* Mol Microbiol, 2016. **101**(6): p. 942-53.
57. Zhang, X., K.W. Bayles, and S. Luca, *Staphylococcus aureus CidC Is a Pyruvate:Menaquinone Oxidoreductase.* Biochemistry, 2017. **56**(36): p. 4819-4829.
58. Pick, T.R., et al., *PLGG1, a plastidic glycolate glycerate transporter, is required for photorespiration and defines a unique class of metabolite transporters.* Proc Natl Acad Sci U S A, 2013. **110**(8): p. 3185-90.
59. Charbonnier, T., et al., *Molecular and Physiological Logics of the Pyruvate-Induced Response of a Novel Transporter in Bacillus subtilis.* mBio, 2017. **8**(5).
60. van den Esker, M.H., T. Kovács Á, and O.P. Kuipers, *YsbA and LytST are essential for pyruvate utilization in Bacillus subtilis.* Environ Microbiol, 2017. **19**(1): p. 83-94.
61. Ahn, S.J., et al., *Characterization of LrgAB as a stationary phase-specific pyruvate uptake system in Streptococcus mutans.* BMC Microbiol, 2019. **19**(1): p. 223.
62. Ahn, S.J., et al., *The Pta-AckA Pathway Regulates LrgAB-Mediated Pyruvate Uptake in Streptococcus mutans.* Microorganisms, 2020. **8**(6).
63. Smith, D.L., et al., *Purification and biochemical characterization of the lambda holin.* J Bacteriol, 1998. **180**(9): p. 2531-40.
64. Brunskill, E.W. and K.W. Bayles, *Identification of LytSR-regulated genes from Staphylococcus aureus.* J Bacteriol, 1996. **178**(19): p. 5810-2.

65. Lehman, M.K., et al., *Identification of the amino acids essential for LytSR-mediated signal transduction in Staphylococcus aureus and their roles in biofilm-specific gene expression.* Mol Microbiol, 2015. **95**(4): p. 723-37.
66. Patton, T.G., S.J. Yang, and K.W. Bayles, *The role of proton motive force in expression of the Staphylococcus aureus cid and lrg operons.* Molecular Microbiology, 2006. **59**(5): p. 1395-1404.
67. Rice, K.C. and K.W. Bayles, *Molecular control of bacterial death and lysis.* Microbiology and Molecular Biology Reviews, 2008. **72**(1): p. 85-+.
68. Rice, K.C., et al., *The cidA murein hydrolase regulator contributes to DNA release and biofilm development in Staphylococcus aureus.* Proceedings of the National Academy of Sciences of the United States of America, 2007. **104**(19): p. 8113-8118.
69. Rice, K.C., et al., *Acetic acid induces expression of the Staphylococcus aureus cidABC and lrgAB murein hydrolase regulator operons.* Journal of Bacteriology, 2005. **187**(3): p. 813-821.
70. Young, R., *Phage lysis: do we have the hole story yet?* Curr Opin Microbiol, 2013. **16**(6): p. 790-7.
71. Young, R., *Phage lysis: three steps, three choices, one outcome.* J Microbiol, 2014. **52**(3): p. 243-58.
72. Savva, C.G., et al., *Stable micron-scale holes are a general feature of canonical holins.* Mol Microbiol, 2014. **91**(1): p. 57-65.
73. Chang, C.Y., K. Nam, and R. Young, *S gene expression and the timing of lysis by bacteriophage lambda.* J Bacteriol, 1995. **177**(11): p. 3283-94.
74. Young, R., *Bacteriophage holins: deadly diversity.* J Mol Microbiol Biotechnol, 2002. **4**(1): p. 21-36.
75. Pang, T., et al., *Visualization of pinholin lesions in vivo.* Proc Natl Acad Sci U S A, 2013. **110**(22): p. E2054-63.
76. Thomas, V.C., et al., *A central role for carbon-overflow pathways in the modulation of bacterial cell death.* PLoS Pathog, 2014. **10**(6): p. e1004205.
77. Yang, Y., et al., *A chloroplast envelope membrane protein containing a putative LrgB domain related to the control of bacterial death and lysis is required for chloroplast development in Arabidopsis thaliana.* New Phytol, 2012. **193**(1): p. 81-95.
78. Nizet, V., *Understanding how leading bacterial pathogens subvert innate immunity to reveal novel therapeutic targets.* J Allergy Clin Immunol, 2007. **120**(1): p. 13-22.
79. Sharma-Kuinkel, B.K., et al., *The Staphylococcus aureus LytSR two-component regulatory system affects biofilm formation.* J Bacteriol, 2009. **191**(15): p. 4767-75.
80. Mates, S.M., et al., *Membrane potential in anaerobically growing Staphylococcus aureus and its relationship to gentamicin uptake.* Antimicrob Agents Chemother, 1983. **23**(4): p. 526-30.
81. Lang, V.J., C. Leystra-Lantz, and R.A. Cook, *Characterization of the specific pyruvate transport system in Escherichia coli K-12.* J Bacteriol, 1987. **169**(1): p. 380-5.
82. Mager, J. and I. Blank, *Synthesis of Fluoropyruvic Acid and some of its Biological Properties.* Nature, 1954. **173**(4394): p. 126-127.
83. Halsey, C.R., et al., *Amino Acid Catabolism in Staphylococcus aureus and the Function of Carbon Catabolite Repression.* mBio, 2017. **8**(1).
84. Görke, B. and J. Stülke, *Carbon catabolite repression in bacteria: many ways to make the most out of nutrients.* Nat Rev Microbiol, 2008. **6**(8): p. 613-24.
85. Kim, H.M., et al., *Regulation of cid and lrg expression by CcpA in Streptococcus mutans.* Microbiology (Reading), 2019. **165**(1): p. 113-123.

86. Cherrington, C.A., et al., *Organic acids: chemistry, antibacterial activity and practical applications.* Adv Microb Physiol, 1991. **32**: p. 87-108.
87. Rottenberg, H., *The measurement of membrane potential and deltapH in cells, organelles, and vesicles.* Methods Enzymol, 1979. **55**: p. 547-69.
88. Krismer, B., et al., *Nutrient limitation governs Staphylococcus aureus metabolism and niche adaptation in the human nose.* PLoS Pathog, 2014. **10**(1): p. e1003862.
89. Jenkins, A., et al., *Differential expression and roles of Staphylococcus aureus virulence determinants during colonization and disease.* mBio, 2015. **6**(1): p. e02272-14.
90. Liebeke, M. and M. Lalk, *Staphylococcus aureus metabolic response to changing environmental conditions - a metabolomics perspective.* Int J Med Microbiol, 2014. **304**(3-4): p. 222-9.
91. Beier, D. and R. Gross, *Regulation of bacterial virulence by two-component systems.* Curr Opin Microbiol, 2006. **9**(2): p. 143-52.
92. Harper, L., et al., *Staphylococcus aureus Responds to the Central Metabolite Pyruvate To Regulate Virulence.* mBio, 2018. **9**(1).
93. Haag, A.F. and F. Bagnoli, *The Role of Two-Component Signal Transduction Systems in Staphylococcus aureus Virulence Regulation.* Curr Top Microbiol Immunol, 2017. **409**: p. 145-198.
94. Saier, M.H., et al., *Catabolite repression and inducer control in Gram-positive bacteria.* Microbiology (Reading), 1996. **142 (Pt 2)**: p. 217-230.
95. Brown, A.F., et al., *Staphylococcus aureus Colonization: Modulation of Host Immune Response and Impact on Human Vaccine Design.* Front Immunol, 2014. **4**: p. 507.
96. DelMain, E.A., et al., *Stochastic Expression of Sae-Dependent Virulence Genes during Staphylococcus aureus Biofilm Development Is Dependent on SaeS.* mBio, 2020. **11**(1).
97. Heim, C.E., et al., *Lactate production by Staphylococcus aureus biofilm inhibits HDAC11 to reprogramme the host immune response during persistent infection.* Nat Microbiol, 2020. **5**(10): p. 1271-1284.
98. Gross, A. and S.G. Katz, *Non-apoptotic functions of BCL-2 family proteins.* Cell Death Differ, 2017. **24**(8): p. 1348-1358.